Neutrino physics at the UNK, Part II[1)]

P. S. Isaev

Joint Institute for Nuclear Research, Dubna

V. A. Tsarev

Physics Institute, USSR Academy of Sciences, Moscow

Fiz. Elem. Chastits At. Yadra **21**, 5–74 (January–February 1990)

The present status of problems in neutrino physics at high energies is analyzed. Possibilities of investigating them in experiments with the neutrino beams at the UNK (the high-energy storage facility at Serpukhov) are considered.

1. NUCLEAR EFFECTS

The investigation of nuclear effects in neutrino interactions is of great interest. Through deep inelastic scattering of neutrinos by nuclei one can investigate nuclear structure, the properties of nuclear forces, the structure of matter at short distances (nucleon correlations, multiquark configurations, the high-momentum isobaric component, etc.). At the same time, one can obtain unique information about QCD phenomena that cannot be recovered within the framework of perturbation theory, namely, phenomena associated with confinement of quarks in a nucleus and in an individual nucleon. It is important to establish whether a nuclear medium possessing a density appreciably lower than the nucleon density can affect the quark–gluon structure of the nucleon. In contrast to relativistic nucleus–nucleus collisions, in which it is supposed that a very high density of the nuclear matter $\rho \sim \Lambda^3 \gtrsim 1$ GeV/F^3 can be attained, the matter densities involved in deep inelastic scattering are characteristic of "cold" nuclei. If M is the nucleon mass, A is the atomic number of the nucleus, and R_A is the radius of the nucleus, then the matter density ρ_A in a nucleus with atomic number A can be estimated at

$$\rho_A \sim \frac{A \cdot M}{\frac{4}{3}\pi R_A^3} \sim 0.14 \text{ GeV/F}^3.$$

Accordingly, for a proton with radius ~ 0.8 F,

$$\rho_p \sim \frac{1 \text{ GeV}}{\frac{4}{3}\pi (0.8 \text{ F})^3} \sim 0.5 \text{ GeV/F}^3.$$

The presence of the nuclear environment may permit the quarks of an individual nucleon to propagate over the space of the nucleus, and this may lead to either partial overlapping of the quark bags of the different nucleons, or to "swelling" of the nucleon in the nuclear medium. In this case the distribution functions of the quarks and gluons in a nucleon within a nucleus will be different from the distribution functions of the quarks and gluons within a free nucleon. In a nucleus, the spectrum of the quarks and gluons will become softer. At the same time, the Fermi motion within the nucleus may have the consequence that a proportion of the quarks and gluons acquire momenta $x \sim 1$. Finally, collective effects may lead to cumulative processes in the region $x > 1$. It is worth noting that it was in fact the cumulative effect which first showed that the nuclear structure function is not a simple sum of the structure functions of the individual nucleons, or equivalently, that the structure functions of the free nucleon and the bound nucleon are different. Indeed, nuclei can be regarded as independent objects for which, just as for hadrons, the structure is characterized at a fundamental level by nuclear structure functions, and the concept of limiting fragmentation is well defined.[1]

Nuclei can be used as "analyzers" of reactions and, above all, of the space-time development of multiparticle production processes. In fact, reactions on nuclei are probably the only way to obtain such information. However, if it is to be extracted from an experiment, we must know how, by appropriate selection of events, to vary the mean distance between nucleons in a nucleus.[2]

A complication of recent measurements of the x dependence of the ratio of the structure functions for heavy nuclei and for deuterium,

$$R\left(\frac{A}{D}\right) = \frac{\frac{d\sigma}{dx}(A)}{\frac{d\sigma}{dx}(D)},$$

is shown in Fig. 1. To discuss the various effects, it is convenient to consider the following regions of x:

a) very small $x (x < 0.1)$, where $R(x) < 1$ as a consequence of nuclear screening ("shadow" effect);

b) small $x (0.1 < x < 0.2)$, where $R > 1$ (antiscreening effect);

c) intermediate $x (0.2 \lesssim x \lesssim 0.7)$, where $R < 1$ and the quark distribution in the nucleons of the nucleus is softer than the distribution in free nucleons;

d) large $x (0.7 \lesssim x \lesssim 1)$, where the behavior of the structure functions is to a large degree determined by the effects of the Fermi motion (and, possibly, multiple scattering);

e) very large $x (x > 1)$, the so-called cumulative region, which is inaccessible for reactions on free nucleons and is governed entirely by collective nuclear effects.

Nuclear structure functions at $x < 1$ and the EMC effect

Screening (or the "shadow" effect) is defined in nuclear physics as the deviation of the cross section from a linear A dependence:

$$\sigma = \sigma_0 A^{\alpha}.$$

If $\alpha < 1$, the effect is called screening; if $\alpha > 1$, antiscreening.

A deviation of α from unity for a nucleus can be due to several factors: binding of the nucleons in the nucleus, overlapping of the parton distributions of the bound nucleons in the nucleus, recombination, and other possible factors.

The early experiments on deep inelastic scattering of

 0090-4759/90/010001-31$04.00

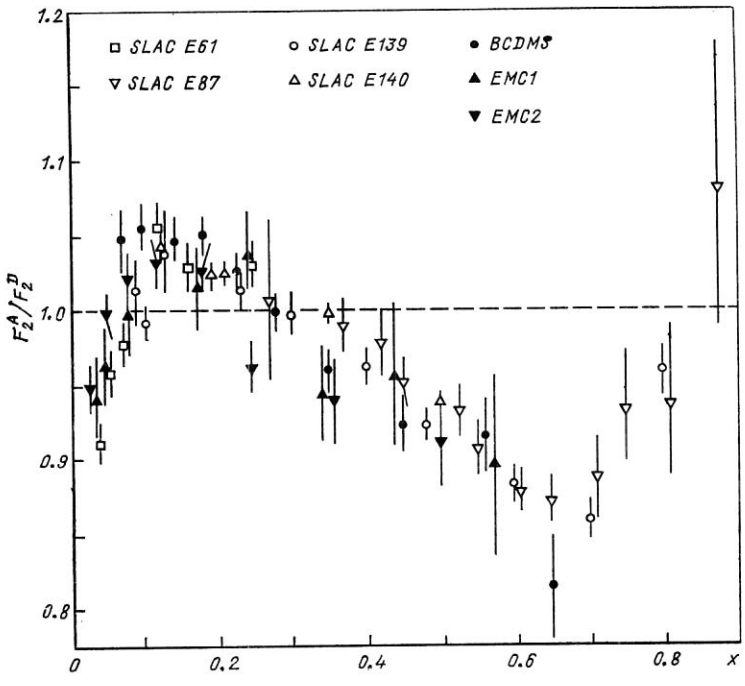

FIG. 1. Compilation of data on ratios of the structure functions of different nuclei.[4]

neutrinos by nuclei did not reveal screening. However, they had poor statistics and low systematic accuracy. Recent experiments with the bubble chamber BEBC and CERN[3] revealed for the first time in neutrino experiments a clear presence of screening in the region of small $x \lesssim 0.15$ and antiscreening in the region $0.15 \lesssim x \lesssim 0.4$ for all Q^2 in the studied range 1–30 GeV^2. The EMC group obtained new interesting data[4] in the region $x < 0.1$, namely, the ratio $F_2^A(x,Q^2)/F_2^D(x,Q^2)$ (Fig. 2) is less than unity and becomes smaller at larger A. Such behavior cannot be explained by the models that are usually employed to interpret the EMC effect. The vector-dominance model leads to such screening for real photons and virtual photons with small Q^2. However, these effects vanish with increasing Q^2 as $1/Q^2$ and must be unimportant for the region studied in the experiment of Ref. 4. A qualitative explanation for the screening at large Q^2 could be provided by the Zakharov–Nikolaev model[5] (see also Ref. 6), in accordance with which the virtual photon "sees" partons distributed in the longitudinal direction in a region $\Delta z \sim 1/Mx$. For $x < x_c A^{-1/3}$, where $x_c \sim m_\pi/M_N \sim 0.15$, the partons belonging to different nucleons overlap in the longitudinal direction. Their fusion leads to screening at $x < x_c$, while momentum conservation leads to a growth of F^A/F^D at $x \sim x_c$ ("antiscreening"). However, this model predicts a stronger A dependence than is found experimentally.

The currently existing neutrino data (Figs. 3–5) do not yet permit a detailed analysis of the deep inelastic scattering of neutrinos. Nevertheless, they permit some important conclusions to be drawn.[3]

1. The ratio of the $\nu N(\bar{\nu}N)$ cross sections determined from interactions with the Ne and D nuclei shows that the fractions of the momenta associated with the gluons and the quarks (calculated per nucleon) are the same for the two targets to within $\pm 4\%$.

2. The ratio of the x distributions for $0.2 \lesssim x \lesssim 0.6$ exhibits the same decrease with x as is observed in the scattering of muons and electrons by the same targets.

If the distributions for the valence (q_v) and sea (q_s) quarks are parametrized in the form

$$q_v = 3x^\alpha (1-x)^\beta;$$
$$q_s = \delta (1+\gamma)(1-x)^\gamma,$$

then the "softening" of the distribution of the valence quarks in neon corresponds to $\beta_{\mathrm{Ne}} - \beta_{\mathrm{D}} \simeq 0.2 \pm 0.1$.

3. The ratio of the y distributions (by means of which the contribution of the sea quarks can be separated) rules out the possibility of any significant growth in the contribution of the "sea" quarks in the nucleus of the kind assumed in some early models of the EMC effect.[7] Such models are also not saved by a variation of $R = \sigma_L/\sigma_T$ with A, since the data indicate the R_{Ne} is close to R_{D}.

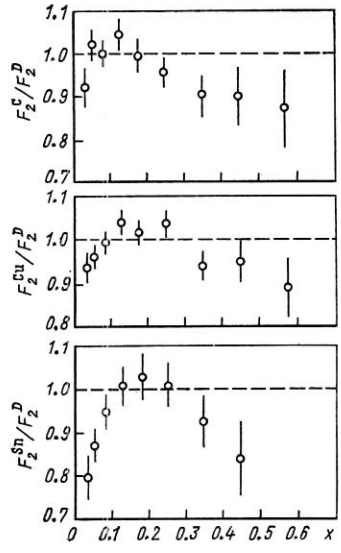

FIG. 2. Ratios of structure functions of the C, Cu, and Sn nuclei to the deuteron structure function as found in the experiment of Ref. 4.

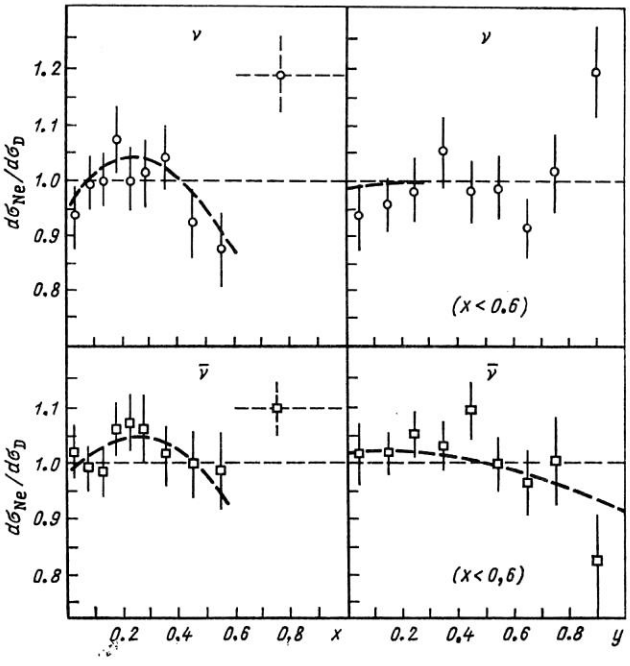

FIG. 3. Ratios of cross sections for neutrino and antineutrino interactions for the nuclei of neon and deuterium (per nucleon) as functions of x and y.[3]

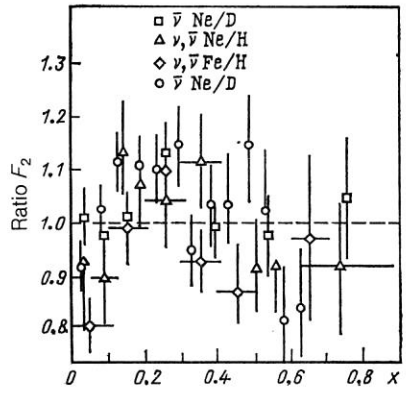

FIG. 5. Compilation of data on the ratio of the structure functions of various nuclei measured in neutrino reactions.

4. The shapes of the distributions for the valence quarks in Ne and D are different: β_{Ne} is greater than β_{D} by 0.5 ± 0.2, and $(\alpha_{\mathrm{Ne}} - \alpha_{\mathrm{D}}) \sim (0.2 \pm 0.1)(\beta_{\mathrm{Ne}} - \beta_{\mathrm{D}})$. At the same time, the shapes of the distributions for the sea quarks in Ne and D differ little ($\gamma_{\mathrm{Ne}} - \gamma_{\mathrm{D}} \sim 1 \pm 1$). The fraction of the "sea" quarks in Ne is smaller than the deuterium by $8 \pm 5\%$ or $18 \pm 8\%$, depending on the model adopted for σ_L/σ_T and $\gamma_{\mathrm{Ne}} - \gamma_{\mathrm{D}}$.

By softening the valence quarks ($\beta \to \beta + \Delta\beta$) and enhancing the contribution of the sea quarks ($s \to R_s s$), one can achieve a good description of the EMC effect for $\Delta\beta = 0.2$ and $R_s = 1.35$ for the neutrino interactions. But this then leads to a y dependence for the antineutrinos in complete conflict with experiment. One could attempt to compensate the enhancement of the contribution of the sea quarks in $\bar{\nu}$ interactions by assuming an increase of $R = \sigma_L/\sigma_T$ for heavy nuclei. But then the y dependence for ν interactions conflicts with experiment. The combination $\nu + (\sigma_{\bar{\nu}}/\sigma_{\nu})\bar{\nu}$, which is not sensitive to the contribution of the sea quarks, is shown in Fig. 4. It can be seen that a deviation from unity, which would indicate an A dependence of R, is not found. Thus, from the neutrino data one can obtain very strong restrictions on the models. The much better statistical and symmetric accuracy in UNK experiments could lead to a fuller understanding of the quark–gluon structure of nuclei and of nucleons and to a test of QCD. In this connection, it would be particularly important to investigate a possible Q^2 dependence of both the screening effects and, in particular, the EMC effect. The existing data do not reveal a strong Q^2 dependence, but the large errors leave great possibilities for contributions that do not satisfy scaling. The identification of such contributions would be important both from the point of view of getting more accurate knowledge about the QCD evolution of the structure functions and for the resolution of the very interesting question of the role of rescaling[8] in nuclei. It would also be interesting to compare the predictions of the various models for the ratio $R_{\bar{q}} = \bar{q}^A(x)/\bar{q}^N(x)$ in the region of large x, where at present there are no data (Fig. 6).

It should be emphasized that the theoretical models of the EMC effect that actually now exist are based entirely on experimental data, and therefore the refinement and extension of these data is of the greatest importance.

In this connection, it is worth mentioning the methodological novelty of the E745 collaboration.[9] Neutrino interaction events were selected by establishing whether or not there were dark tracks at the interaction point. The basic idea of the method is the assumption that neutrino interactions with surface nucleons of a nucleus and with nucleons situated "within" a nucleus may be distinguished by the nuclear fragments. It is assumed that events with dark tracks are due to interactions with "internal" nucleons, while events without dark tracks are attributed mainly to interactions of neutrinos with surface nucleons. Of course, this is not absolutely accurate, but in a "first approximation" the assumption is justified. The new method may, in the opinion of the authors, case light on the physical reason for the behavior of the cross-section ration $F_2^A(x,Q^2)/F_2^D(x,Q^2)$ in the region $x \gtrsim 0.7$.

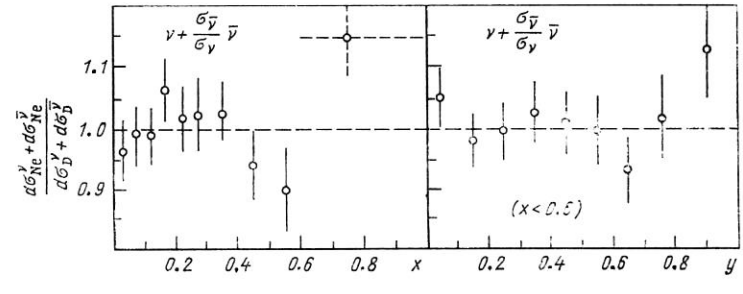

FIG. 4. The ratio $(d\sigma^{\nu}_{\mathrm{Ne}} + d\sigma^{\bar{\nu}}_{\mathrm{Ne}})/(d\sigma^{\nu}_{\mathrm{D}} + d\sigma^{\bar{\nu}}_{\mathrm{D}})$ as a function of x and y.[3]

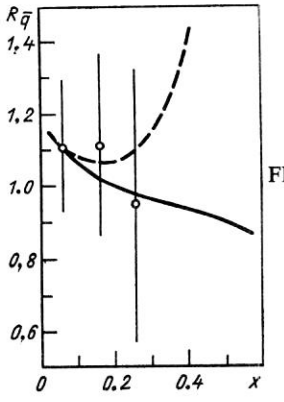

FIG. 6. The value of $R_{\bar{q}}$ as a function of x.

Cumulative processes

Cumulative production of particles, i.e., production in a kinematic region forbidden for the free nucleon, and the intimately related phenomenon of limiting fragmentation of nuclei were first discovered in experiments performed at the Joint Institute for Nuclear Research and the Institute of High Energy Physics at Serpukhov (see the reviews of Ref. 1) and have meanwhile been studied in some detail in hadron and photon processes. The information obtained in neutrino reactions is considerably sparser, both in volume and variety and in statistical and systematic accuracy.

The great interest in cumulative processes is due in the first place to their possible connection with nontrivial features of the internal structure of nuclei such as correlations of groups of nucleons, multiquark formations like fluctons, or possibly even a quark–gluon phase of nuclear matter. This suggests that there could be an intimate connection between cumulative processes and the EMC effect, which could be manifestations of a quark–gluon degree of freedom in different kinematic regions.[10] A different point of view is that the cumulative processes reflect not so much details of the internal structure of nuclei as the interaction of fast particles with nuclear targets. An excited system could be formed in the interaction process and become a source of cumulative particles.[11]

As in the case of the EMC effect, numerous theoretical models have been proposed for the cumulative effect. These range from ones that take into account the fairly trivial processes of multiple scattering and cascading to quite sophisticated models that take into account the formation of multiquark configurations and rescaling.

In particular, Zotov *et al.*[12] proposed a fluctón nuclear model with rescaling, in the framework of which they successfully reproduced experimental observations: the softening of the parton distribution at small values of x and the presence of partons in the region $x > 1$. They calculated cross sections for the production of massive lepton pairs on different nuclei. They predicted x, Q^2, and A dependences of the nuclear structure functions in the cumulative region $x > 1$. However, as in the case of the EMC effect, there is as yet no single viewpoint with regard to the fundamental mechanism of the cumulative effect.

Analysis of experimental data on production of cumulative nucleons on Ne nuclei in antineutrino beams (Fermilab[13]) lent support to breaking of pairing correlations[2] as the source of cumulative protons. In this model the large value of $\alpha = (E - p\cos\theta)/m$ of a cumulative proton emitted backward is compensated by the momentum of a nucleon emitted forward. The "Doppler effect" leads to a lowering of the mean x and to an α dependence

$$\langle x_\alpha \rangle = (2 - \alpha)\ \langle x \rangle,$$

where x_α corresponds to events with cumulative protons. The data of Ref. 13 do not contradict such a dependence. However, such a dependence was not observed in an experiment using the SKAT chamber[14] (Fig. 7). At the same time, facts were discovered that the authors interpreted as support for the mechanism of secondary rescattering as the source of the cumulative protons. The important part played by the absorption of slow pions, $\pi + 2N \to 2N$, the cross section of which has a maximum at momentum $p_\pi \approx 0.25$ GeV/c, was also emphasized.

However, it must be borne in mind that the existing data have a rather low statistical accuracy ($\lesssim 10^3$ events) and are subject to the strong influence of the systematic uncertainty in the knowledge of the energies of the initial neutrinos. As a result, in the experiment of Ref. 14, for example, the angle between the true and the experimentally determined direction of the momentum-transfer vector $\mathbf{q} = \mathbf{p}_\nu - \mathbf{p}_\mu$ is 20–40°. In addition, the poor statistics did not permit advance into the region of large $x(>2)$, where there is a particular sensitivity to the mechanisms of cumulative production.

Experiments at the UNK will make it possible to eliminate these shortcomings, to improve the accuracy of the measurements, and the advance into the region of large x, where it should be possible to test the predictions[10] about the possible reflections of the EMC effect in the cumulative region in the form of an irregular (step) behavior of $R(x)$ at $x > 1$. An indication of such behavior has been obtained in hadronic and electromagnetic cumulative reactions (Fig. 8).

Space-time evolution of the final system

Study of the development in space and time of the final hadronic system produced in a high-energy collision of particles is one of the most important tasks of modern high-energy physics. Nuclear targets in which the internucleon distances are of the same order as (or less than) the characteristic spatial scales of the development of the system give a unique possibility for such investigations.

The existence of a "formation length" is well known and reliably established in electrodynamics and is also assumed in hadrodynamics. On the basis of the parton model it

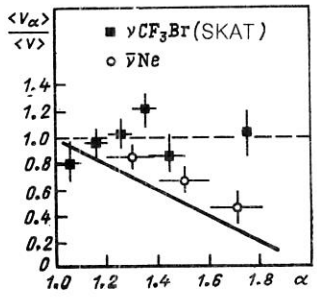

FIG. 7. The mean value $\langle \nu_\alpha \rangle / \langle \nu \rangle$ for events having one cumulative proton as a function of $\alpha = (E - p_x)/M$. The results of experiments in bubble chambers with CF_3Br and Ne filling are shown; the continuous line shows the predictions of a model of two-particle correlation.

is assumed that secondary hadrons with energy E are formed at a distance $l(E) \simeq E/\mu^2$ from the target,[15] where μ is some characteristic hadron mass. The slowest of the partons belonging to a composite quark is the first to interact with the target, and the first hadron is produced. The disruption of the coherence of the parton system leads to the decay (and subsequent hadronization) of the parton with the next rapidity, etc. the fast partons have a small cross section for interaction with the target and can participate in the interactions only when they have been slowed down by degradation of the momenta (which accompanies their decay).

In contrast to the parton picture based on models of the $\lambda\varphi^3$ type, in QCD the gluon spin, which is equal to unity, leads to an interaction cross section that does not decrease with the energy, as a result of which the fast composite quark can repeatedly interact in the nucleus with a large cross section [$\sim(1/3)\sigma_{NN}$]. As a result of the interaction between an incident quark and a target quark, a string is stretched and, after breaking, gives secondary hadrons. As was noted in Ref. 16, the spectra predicted by the ordinary parton model and by the QCD model are different. In particular, the ratio of the spectra R_y on a nucleus and on a nucleon does not have a minimum in the region $y \lesssim y_A = \ln \mu^2 Z_A/\langle m_I \rangle$, and in R_y there is no plateau separating the region of beam fragmentation from the cascade region.

In the framework of the formation-length hypothesis, hadrons are formed at large momenta outside the nucleus, and this may be important for the development of the intranuclear cascade. Neutrino reactions on nuclei permit a direct test of this phenomenon. Experimental data on charged-current ν_μ interactions were analyzed in Ref. 17. A model of an intranuclear cascade in which the effect of formation of secondary particles was introduced was used. The parameter μ^2 was determined by comparison with the experimental multiplicity of slow secondary protons ($0.3 < p < 0.6$ GeV/c), which is most sensitive to the number of intranuclear collisions. As can be seen in Fig. 9, the best agreement with experiment occurs for $\mu^2 = (0.08^{+0.05}_{-0.04})$ GeV$^2/c^4$. This result agrees with the estimates obtained in hA (Ref. 18) and νA (Ref. 19) interactions, but does not agree with the values $\mu^2 \sim 0.5$–0.7 GeV$^2/c^4$ found from hA interactions in Ref. 20.

In experiments with nuclear targets at the UNK it will be possible to investigate in more detail the space-time development of the hadronic system produced in neutrino processes and make comparisons with the results of investigations for hadronic and electromagnetic processes. At the same time, it is possible to exploit the possibility, noted by Baldin,[1] of selecting events with the participation of nucleons at short distances by means of cumulative processes.

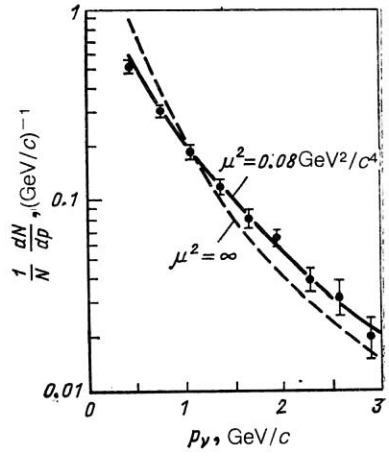

FIG. 9. Pulse spectrum of negative mesons. The curves are the results of calculations in accordance with the cascade model with $\mu^2 = \infty$ and $\mu^2 = 0.08$ GeV$^2/c^4$.

Nuclear enhancement of processes with large p_T

There is special interest in the study of reactions on nuclei that lead to the production of particles with large transverse momenta. As was first found in Ref. 21, the cross sections of such processes vary as A^α with $\alpha > 1$. The main mechanisms are evidently: a) multiple soft scattering by many nucleons of the nucleus;[22] b) hard scattering of constituents accompanied by the production of jets with large values of the transverse energy E_T.[23] Figure 10 shows the results of a recent experiment on the Tevatron[24] at energy $E_p = 800$ GeV for the dependence of the exponent α on E_T and on the planarity

$$P = \max \frac{\sum p_{iL}^2 - \sum p_{iT}^2}{\sum p_{iL}^2 + \sum p_{iT}^2},$$

where p_{iT} and p_{iL} are, respectively, the perpendicular and parallel components of the transverse momentum of the particle with respect to an arbitrary axis in the transverse plane. Note that in the limit $P \to 1$ the value of α decreases to unity, which indicates a contribution of hard collisions leading to jet production. So far as we know, no detailed investigations

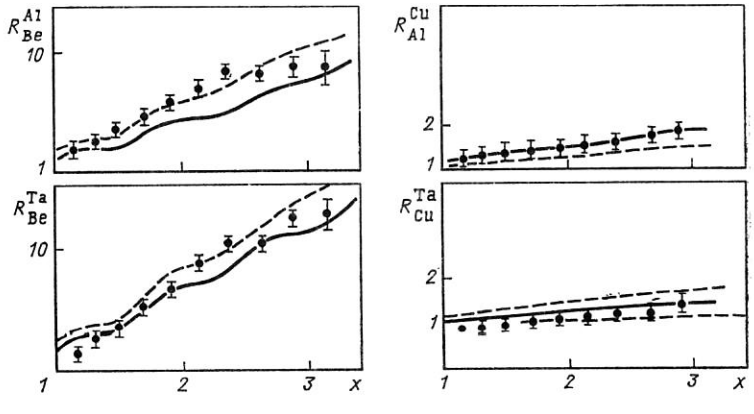

FIG. 8. The ratio $R_{A_2}^{A_1} = A_2 F_2^{A_1}/A_1 F_2^{A_2}$ as a function of x for various nuclei. The scale of the ordinate is logarithmic.

of this effect for neutrino reactions have been made. The UNK neutrino beams and detectors will permit such investigations and will yield important information about the processes that occur in interactions with nucleons and nuclei.

2. SEARCHES FOR NEW PHYSICS

The well-known graph of the variation of the constants of the strong, electromagnetic, and weak interactions with increasing energy demonstrates the unification of all interactions. Theoretical estimates show that the grand-unification scale lies in the region of 10^{15} GeV (Fig. 11). In the minimal $SU(5)$ grand-unification theory it was assumed that the region of energies above 100 GeV will be a "desert" unpopulated by the masses of new elementary particles. However, it was soon shown that the proton lifetime is longer than that predicted by the $SU(5)$ theory by at least 2–3 orders of magnitude, and the "desert" could be populated by new particles corresponding to supersymmetric (SUSY) models. The mass scale of the superparticles (or "sparticles," as they are called) could well be situated at about 1 TeV. Supersymmetry is a new form of symmetry that relates bosons to fermions. Supersymmetries are characterized by a number N. If $N = 1$, then the supersymmetry is said to be simple; if $N > 1$, the supersymmetry is said to be extended.[25,26]

For clarity, we give in Table I the minimal set of supersymmetric particles present in any supersymmetric model of simple supersymmetry ($N = 1$). Here, the leptons and quarks are fundamental particles possessing scalar left and right partners. In the group of gauge particles (gauginos) each massless gauge boson is associated with one Majorana

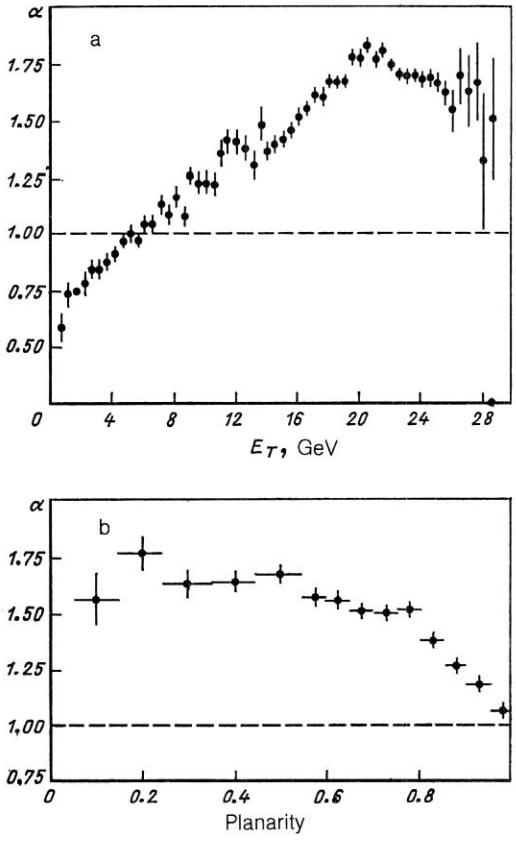

FIG. 10. Dependence of the exponent α on E_T (a) and the planarity (b).

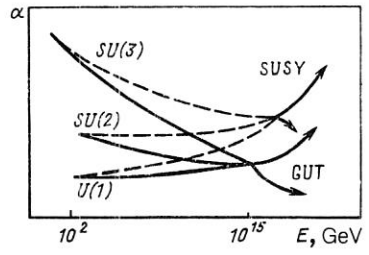

FIG. 11. Graph of unification of the coupling constants of the strong, electromagnetic, and weak interactions.

and gauge fermion (to the photon γ there corresponds the photino $\tilde{\gamma}$, and to the gluon g, the gluino $\tilde{g}$). To the neutral massive gauge boson Z^0 there correspond two Majorana gauge fermions Z_1^0 and Z_2^0 and one Higgs scalar boson H_Z^0. To the charged $W^{\pm}$ boson there correspond two Dirac fermions $W_1^{\pm}$ and $W_2^{\pm}$ and a charged Higgs scalar boson H_W. There are also at least two neutral Higgs bosons, the scalar H_0 and the axial pseudoscalar A^0, which correspond to a Majorana fermion, the higgsino H^0. The gravitino $\tilde{G}$ corresponds to the graviton G.

Supersymmetry is realized either globally or locally with allowance for supergravity. In the first case, the breaking of supersymmetry is associated with the formation of a goldstino $\mathscr{G}$, and in the second case with the formation of the gravitino $\tilde{G}$. The mass spectrum of the supersymmetric particles is unknown, and this makes a search for them difficult. Estimates of their masses can be obtained from a calculation of the radiative corrections to the masses of, for example, the scalar bosons in the standard model, such as the Higgs boson:

$$\delta M_H^2 = O\left(\frac{\alpha}{\pi}\right)\Lambda^2,$$

where Λ is the cutoff constant in the divergent loop. If we make the "natural" assumption that the physical mass of the Higgs boson must not be significantly greater than the mass of the W boson ($M_H^2 \approx M_W^2$) and that the correction δM_H^2 must not be greater than the mass M_H^2 itself, then this relation shows that the value of Λ is $\lesssim 1$ TeV. This problem of naturalness[25] can be successfully solved in the framework of supersymmetry.

In supersymmetric theory, the quadratically divergent boson and fermion loop corrections to M_H^2 have opposite signs, and since the bosons and fermions occur as pairs with equal values of coupling constants, the divergences in δM_H^2 will cancel:

$$\delta M_H^2 = O\left(\frac{\alpha}{\pi}\right)|M_B^2 - M_F^2|.$$

The remaining finite mass difference of the boson and fermion superpartners is proportional to the scale of the supersymmetry breaking. The cutoff constant Λ is equivalent to a mass difference $|M_B^2 - M_F^2| \lesssim 1$ (TeV/c^2)^2, and since one of the masses is known from the standard model and the second is supersymmetric, it is concluded that the supersymmetric partners of the known particles must have masses $\lesssim 1$ TeV/c^2.

The expected masses of the supersymmetric particles are given in Table II. If the mass limit for the Higgs boson is shifted to ≈ 300 GeV/c^2, we obtain the following mass esti-

TABLE I. Minimal set of supersymmetric particles (supersymmetric theory with $N = 1$).

Spin 0	Spin 1/2	Spin 1	Spin 3/2	Spin 2
	Goldstino $\mathscr{G}$		Gravitino $\tilde{G}$	Graviton G
Scalar neutrino $\tilde{\nu}$	Neutrino ν			
Scalar leptons $\tilde{l}_R, \tilde{l}_L$	Leptons l			
Scalar quarks $\tilde{q}_R, \tilde{q}_L$	Quarks q			
	Gauginos: Photino $\tilde{\gamma}$; Gluino $\tilde{g}$; Winos $\tilde{W}_1^{\pm}, \tilde{W}_2^{\pm}$; Zinos $\tilde{Z}_1^0, \tilde{Z}_2^0$	Photon γ; Gluon g; $W^{\pm}$ boson; Z^0 boson		
Neutral Higgs boson H_Z^0				
Charged Higgs boson $H_{\tilde{W}}^{\pm}$	Charged higgsino $\tilde{H}^{\pm}$			
Axionlike pseudoscalar A^0	Neutral higgsino $\tilde{H}^0$			
Scalar Higgs boson H^0				

mates for the supersymmetric particles: wino mass ~ 90 GeV/c^2, mass of the leptons ~ 150–200 GeV/c^2, gluino mass ~ 300 GeV/c^2, and mass of the quarks ~ 600 GeV/c^2. If supersymmetric particles are not found within these limits, serious objections to supersymmetry may arise.[26]

The ordinary gauge and Yukawa forms of coupling of the known particles in the standard model have correspondences with the couplings of their supersymmetric partners:[27-29]

$$g\bar{f}\gamma_\mu V^\mu f \to \sqrt{2}\, g f \tilde{V} \tilde{f} + \text{h.c.},$$
$$g\tilde{f}^* \overleftrightarrow{\partial_\mu} \tilde{f} V^\mu, \left(\frac{g}{2}\right)^2 |\tilde{f}^* \tilde{f}|^2,$$
$$\lambda \bar{f} f H \to \lambda f \tilde{f} \tilde{H} + \ldots, \quad \lambda^2 [|\tilde{f}^c \tilde{f}|^2 + |\tilde{f}^c H|^2 + |\tilde{f}^c H|^2].$$

The interactions of the supersymmetric particles are expressed in such a way as to ensure conservation of a new multiplicative quantum number: the R parity. For the standard particles, the R parity is defined to be $+1$, and for their supersymmetric partners to be -1. The R parity is related to the quantum numbers conserved in the standard model by

$$R = (-1)^{B+3L+2S},$$

where B, L, and S are the baryon and lepton numbers and the strangeness, respectively.

Conservation of R partity leads to three important phenomenological consequences:

1) supersymmetric particles are always produced in pairs, for example, $e^+ e^- \to \tilde{\mu}^+ \tilde{\mu}^-$, $p\bar{p} \to (\tilde{g}\tilde{g}$ or $\tilde{q}\tilde{\bar{q}}) + X$, etc.);

2) each particle decays into a different sparticle (for example, $\tilde{e} \to e + \tilde{\gamma}$, $\tilde{g} \to \bar{q}\tilde{q}$, $\tilde{g} \to \bar{q}q\tilde{\gamma}$, $\tilde{q} \to q + \tilde{g}$, etc.);

3) the lightest sparticle in absolutely stable, since it does not have an admissible decay scheme.

Since the lightest sparticle is absolutely stable, it must be present today in large quantities in the universe as a cosmological fossil from the big bang. However, such a sparticle has not yet been observed. Obviously, it must be neutral and colorless, and its interaction must be significantly weaker than the strong and electromagnetic interactions, so that it can escape observation like the ordinary neutrino. Candidates for the sparticle are the gravitino, photino, zino, higgsino, or a scalar neutrino. One of the candidates for the sparticle could be the supersymmetric τ neutrino.[30] If there is a Majorana component of the zino with mass $M \leqslant 3.5$ GeV/c^2, then there must exist a stable supersymmetric τ neutrino with mass $m_\tau < m_{\nu_\tau} \leqslant 3.5$ GeV/c^2. These are more reliable limits on the mass of the sparticle than the limits for the stable higgsino or photino ($m_{\tilde{g}} > 80$ GeV/c^2, as follows from analysis of the data of Ref. 31).

The schemes of direct production of supersymmetric quarks, photinos, gluinos, winos, zinos, and Higgs bosons in neutrino interactions are shown in the diagrams of Figs. 12–15. However, it follows from the restrictions of the masses of the supersymmetric particles obtained by the CELL collaboration (Ref. 32, Fig. 16) that the search for supersymmetric particles in νe or νN collisions at the UNK has no prospects, since even at the maximal energy of the neutrino beam, $E_\nu \sim 2$ TeV, the energy in the neutrino–nucleon center-of-mass system will be $\sim \sqrt{2M_N E_\nu} \leqslant 65$ GeV, a value that lies at the limit of the possible pair-production threshold

TABLE II. Masses of supersymmetric particles, normalized to the mass scale $m_{1/2}$ (Ref. 26).

$\tilde{q}$ quark	$\tilde{g}$ gluino	$\tilde{l}_L \tilde{l}_R$ leptons		$\tilde{W}$ wino	$\tilde{Z}$ zino
1.9	1	0.7	0.4	0.3	0.16

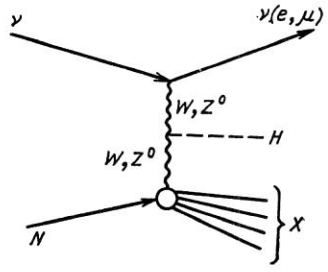

FIG. 12. Production of the Higgs boson in νN interactions.

(supersymmetric particles must be produced in pairs!) of the particles with the lowest masses (Fig. 16). It will be only in interactions of high-energy neutrinos ($E_\nu \gtrsim 1$ TeV) with heavy nuclei ($A \gtrsim 100$), when the energy in the neutrino–nucleus center-of-mass system may reach values $\gtrsim \sqrt{2M_A c^2 E_\nu} = \sqrt{200 \cdot 100} \gtrsim 450$ GeV, that pair production of supersymmetric particles (or of heavy leptons) will be possible. But even in this case additional factors (phase factor, propagators of the heavy superparticles, additional powers of the coupling constants, the small fraction of quarks in a nucleus with large $x \gg 1$) will greatly reduce the cross section for production of the supersymmetric particles, reducing the search for supersymmetric particles in the neutrino beam of the UNK almost to a hypothetical search. Later, we shall devote a full section to the problem of observing supersymmetric particles at the UNK.

Supersymmetry is one of the possible ways of going beyond the standard model. Another possibility is the hypothesis of a composite structure of the elementary particles. In contrast to supersymmetry, this subject is more difficult for theoretical discussion, since there are too many models (as many models as authors). The only thing that they have in common is the method used to parametrize the terms of the Lagrangian in reciprocal powers of Λ, where Λ is the energy scale at which the composite nature of the particles first appears. Such terms are usually expressed in the form

$$\sim \frac{\lambda_{1234}^2}{\Lambda^2} (\bar{\psi}_1 \Gamma \psi_2)(\bar{\psi}_3 \Gamma \psi_4) + O\left(\frac{1}{\Lambda}\right)^3.$$

Some very general requirements are imposed on the four-fermion interaction (for example, it must meet the requirement of color confinement, flavor symmetry, etc.). Terms $\sim (1/\Lambda)^n$ may, in particular, appear in phenomena like flavor-changing neutral currents. The current restrictions on the values of Λ from various processes are given in Table III.

A final possibility is a "minimal" extension of the standard model by the introduction of massive neutrinos, new families of quarks and leptons, and additional gauge bosons.

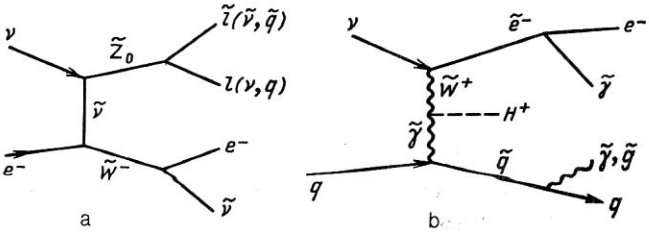

FIG. 13. Production of: a) zino and wino in ve^- collisions; b) charged Higgs boson and supersymmetric particles in νN interactions.

FIG. 14. Production of a $\tilde{\nu}\tilde{e}$ pair in ve^- collisions.

The radiative corrections that arise from the new, as yet unknown, particles may change the predictions of the standard model and indicate new physics.

In this review we devote our main attention to the minimal extension of the standard model, since it corresponds closest to the energy scale of fixed-target experiments at the UNK.

Production and decay of massive neutrinos

Theoretically, massive neutrinos can be obtained by means of the seesaw mechanism of the left–right symmetric model,[33] in models of horizontal gauge symmetry,[34] in the superstring E_6 model,[35] and in a number of other models.

If massive neutrinos ν_H ($\nu_1, \nu_2, \nu_3, \ldots$) exist, they need not be identical to eigenstates ($\nu_e, \nu_\mu, \nu_\tau, \ldots$). It is more likely that there are linear combinations

$$\nu_l = \sum U_{eH} \nu_H \quad (l = e,\ \mu,\ \tau \ldots;\ H = 1,\ 2,\ 3 \ldots),$$

where U_{l_H} is an element of a mixing matrix (a unitary matrix). The constant of the coupling of the charged current of the massive neutrino ν_H to the charged lepton l is proportional to the square of the matrix element. Thus, the leptonic current must contain, besides the terms $(\bar{\nu}_e e)$ and $(\bar{\nu}_\mu \mu)$, the terms $(\bar{\nu}_H e)$ and $(\bar{\nu}_H \mu)$, which will lead to the decays π, $K \to \nu_H + (e,\mu)$. Ordinary neutrino beams (ν_e and ν_μ) may contain an admixture of massive neutrinos, the fraction of which is determined by the decay branching ratio

$$R_H = \frac{\Gamma(h \to \nu_H l)}{\Gamma(h \to \nu_\mu \mu)} = |U_{lH}|^2 \rho_{lH}.$$

Here, ρ_{l_H} is a kinematic factor that depends on m_{ν_H}, and U_{l_H} is an element of the mixing matrix. (There are models[36] in which the interaction of the heavy neutrinos in the neutral-current channel can change their flavor. In this case there may be other contributions to the mixing different from the matrix element U_{l_H}.)

In the case of purely leptonic decay, the kinematic factor ρ_{l_H} takes into account the fact that for a finite mass of the ν_H the suppression due to helicity conservation will be less than for $m_\nu = 0$ [for example, with $m_{\nu_H} = 200$ MeV/c^2 we have $\rho \approx 10^5$ for $K \to e\nu$ and $\rho \approx 10$ for $K \to \mu\nu$ (Ref. 37)].

If ν_H neutrinos arise from the decay of K mesons, then

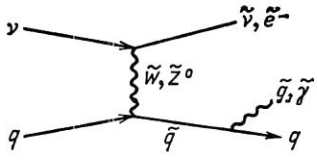

FIG. 15. Production of supersymmetric $\tilde{\nu}$, $\tilde{e}^-$, $\tilde{g}$, and $\tilde{\gamma}$ particles in νN interactions.

TABLE III. Estimates of the values of Λ from different processes.[147]

Чете Four-fermion ный operator	Process	Lower bound on Λ, TeV
$\bar{e}\bar{d}\bar{u}u$	Proton decay	$\lambda \cdot 10^{13}$
$\bar{s}d\bar{s}d$	K^0–$\bar{K}^0$ mixing	$\lambda \cdot 400$
$\bar{c}u\bar{c}u$	D^0–$\bar{D}^0$ mixing	$\lambda \cdot 50$
$\bar{s}d\bar{e}\mu$	$K^+ \to \mu^+\mu^-e^+$	$\lambda \cdot 50$
	$K_L \to \mu e$	$\lambda \cdot 30$

the investigated mass region lies within the limits $m_0 \leqslant m_{\nu_H} \leqslant 490\ \text{MeV}/c^2$, where m_0 is determined by the efficiency with which the ν_H decay through the given channel is detected. For $\pi^+ \to \mu + \nu_H$ the upper limit for the mass is $m_{\nu_H} = 34\ \text{MeV}/c^2$. In the case of the decay of the τ lepton, the mass region of the heavy neutrinos is increased. For example, for the $\tau \to 3\pi\nu_\tau$ channel it reaches $m_{\nu_H} \approx 1.37\ \text{GeV}/c^2$.

Heavy neutrinos can also be produced in a beam of ordinary ν_μ and ν_e through the flavor-changing neutral current:

$$\nu_{\mu,e} + N \to \nu_H + X.$$

In this case the upper limit on the masses is determined solely by the energy of the initial neutrinos.

It is convenient to look for heavy neutrinos in experiments of the beam-dump type, in which the background from the decays of π and K mesons to the ν_e and ν_μ channels is suppressed by 3–4 orders of magnitude. At the same time, a flux of new neutrinos, for example, ν_τ, may arise from semileptonic decays of charmed quarks produced in proton–nucleus interactions and not subject to suppression on account of their short lifetime. For example, in one of its recent experiments the CHAR collaboration[38] looked for heavy neutrinos produced when a beam with proton energy 400 GeV passed through copper (beam-dump experiment). It was assumed that the heavy neutrinos arise through mixing after decay of charmed D mesons. The collaboration looked for ν_H decays in accordance with the schemes

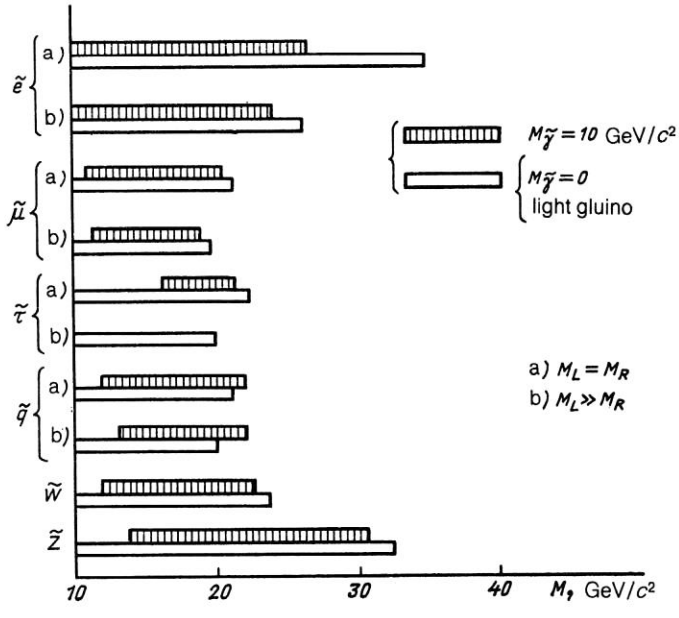

FIG. 16. Regions of masses of supersymmetric particles ruled out at the 95% level.

$$\nu_H \to e^+e^-\nu_e, \quad \mu^+\mu^-\nu_\mu, \quad e^+\mu^-\nu_e, \quad \mu^+e^-\nu_\mu$$

(and the corresponding channels for the antineutrinos). No single candidate was found. The bounds $|U_{l_H}|, |U_{\mu_H}| < 10^{-7}$ on the matrix elements were obtained for neutrino masses of $\sim 1.5\ \text{GeV}/c^2$.

Searches for heavy neutrinos have also been made in a beam with a broad neutrino spectrum. It was assumed that neutrinos are produced in interactions as a result of the neutral current in the CHARM calorimeter. In this case searches were made in the decay channels

$$\nu_H \to \mu + \text{hadrons}.$$

Heavy neutrinos were not found.

This experiment was sensitive to the region of masses

$$0.5 < m_H < 2.8\ \text{GeV}/c^2$$

and gave the bound $|U_{\mu_H}| < 3 \times 10^{-4}$ for a mean mass value 2.5 GeV/c^2 (Ref. 38). Let us consider other possible ν_H decay schemes.

a) The radiative decays $\nu_H \to \nu\gamma, \nu\gamma\gamma$.[39–41] It can be assumed that the neutrino states ν_e, ν_μ, and ν_τ are not states with proper mass and can be expressed in terms of linear combinations of massive neutrino states ν_H. The neutrinos may be Dirac and Majorana states. If such a mixture of states exists, radiative decays, $\nu_j \to \nu_i\gamma$, where $m_{\nu_j} > m_{\nu_i}$ are possible. If $m_{\nu_H} < 2m_e$, the single-photon decay scheme must be preferred. For Dirac neutrinos, the $\nu_H \to \nu_i\gamma$ decay width can be expressed by[42]

$$\Gamma^D \approx \frac{\alpha}{2}\left[\frac{3G_F}{32\pi^2}\right]^2\left[\frac{m_H^2 - m_i^2}{m_H}\right]^3 (m_H^2 + m_i^2)\left(\sum_a U_{ia}^* U_{Ha} r_a\right)^2,$$

and for Majorana neutrinos by[43]

$$\Gamma^M_{(\eta_H = \eta_i)} \approx \frac{9\alpha}{2^{10}}\frac{G_F^2}{\pi^4}\left[\frac{m_H^2 - m_i^2}{m_H}\right]^3$$

$$\times (m_H - m_i)^2\left(\sum_a U_{ia}U_{Ha}r_a\right)^2;$$

$$\Gamma^M_{(\eta_H = -\eta_i)} \approx \frac{9\alpha}{2^{10}}\frac{G_F^2}{\pi^4}\left[\frac{m_H^2 - m_i^2}{m_H}\right]^3$$

$$\times (m_H + m_i)^2\left(\sum_a U_{ia}U_{Ha}r_a\right)^2,$$

where m_H and m_i are the masses of the initial neutrino and the final neutrino, $r_a = (m_{l_a}/M_W)$, m_{l_a} is the mass of a lepton of generation a, are η_H and η_i are the C numbers of the initial and final Majorana neutrinos, respectively.

These relations show that if the neutrino masses have reasonable values, the corresponding lifetime is greater than

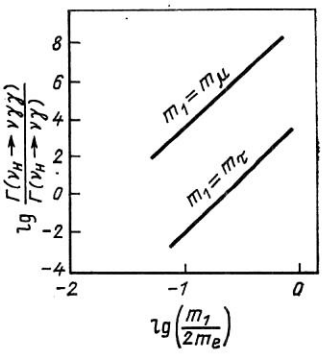

FIG. 17. Ratio of decay widths as a function of the mass m_1 for a Dirac neutrino ($m_\nu = 0$).[41]

the age of the universe, and this is exploited in the construction of various astrophysical hypotheses about the evolution of the universe. Besides the decay $\nu_H \to \nu_i \gamma$, there may also exist the decay $\nu_H \to \nu_i \gamma\gamma$, which must be suppressed by a factor α/π on account of the additional electromagnetic vertex. However, such a naive estimate may be incorrect in the region of masses of the initial neutrinos in which we are interested. In the standard model, the leptonic GIM mechanism[44] suppresses the amplitude of the $\nu_H \to \nu_i \gamma$ decay by the factor

$$\sum_a U^*_{ia} U_{Ha} \left(\frac{m_{la}}{M_W}\right)^2.$$

For the lepton masses known to us, $(m_{la}/M_W)^2 \ll 1$. It was found that for the $\nu_H \to \nu_i \gamma\gamma$ decay the factor $(m_{la}/M_W)^2$ is replaced by the ratio of the lepton masses. This effect may compensate the additional factor α/π and make $\Gamma(\nu_H \to \nu_i \gamma\gamma)$ greater than $\Gamma(\nu_H \to \nu_i \gamma)$. A graph of the ratio $\Gamma(\nu_H \to \nu_i \gamma\gamma)/\Gamma(\nu_H \to \nu_i \gamma)$ is shown in Fig. 17 (taken from Ref. 41).

For $m_{\nu_H} \sim 50$ eV/c^2, the two-photon decay channel is negligibly weak compared with the single-photon channel; for $m_{\nu H} \simeq 2m_e$, the two-photon channel is dominant. For example, for $m_{\nu_H} \simeq 1$ MeV/c^2 we have $\Gamma(\nu_H \to \nu_i \gamma\gamma) \sim (2 \times 10^3 \text{ yr})^{-1}$, whereas $\Gamma(\nu_H \to \nu_i \gamma)$ is three orders of magnitude smaller. For $m_{\nu_H} > 2m_e$ the $\nu_H \to \nu + e^+ + e^-$ decay channel dominates over the radiative (single- or two-photon) channel.[9] Note that all these estimates can be strongly changed if the mixing effect is taken into account. The decay $\nu_H \to \nu_i + 2\gamma$ (the indices H and i relate to the families of leptons) is controlled by the coupling of the lightest lepton, whereas $\nu_H \to \nu_i + \gamma$ is controlled by the coupling of the heaviest lepton. If ν_H and ν_i are not strongly coupled to the τ lepton, then two-photon decay becomes more important for $m_{\nu_H} < 0.2$ MeV/c^2 (Ref. 40).

If $m_{\nu_H} > 2m_e + m_{\nu_i}$, then the decay $\nu_H \to \nu_i + e^+ e^-$ (Fig. 18) becomes dominant. But if for any reason the matrix elements vanish, $U_{l\nu_H}$ or (and $U_{l\nu_i} = 0$, decay process in accordance with this scheme does not occur, and the radiative decays again become dominant.

b) Semileptonic decays $\nu_H \to l^- \pi^+$.

In the region of masses $160 < m_{\nu_H} < 490$ MeV/c^2 the decay $\nu_H \to e^- \pi^+$, to which the diagram in Fig. 19 corresponds, must be dominant. The decay width is

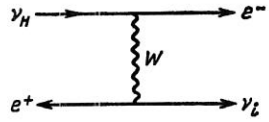

FIG. 18. Decay $\nu_H \to \nu_i + e^+ + e^-$.

$$\Gamma(\nu_H \to e^- \pi^+) \approx 67.1 \left[1 - \left(\frac{m_\pi}{m_{\nu_H}}\right)^2\right]^2 m^3_{\nu_H} |U_{lH}|^2.$$

The dependence of the ν_H lifetime on m_{ν_H} for the different decay channels is shown in Fig. 20 (Ref. 45).

In experiments that look for decays of heavy neutrinos, it must be borne in mind that the ν_H may decay before they reach the detector. if the detector is at an appreciable distance, this can impose restrictions on the sensitivity of the experiment (for large mixings) at low masses.

The topology for the $\nu_H \to + e^+ e^- \nu_e$ decays has the shape of two showers formed in the region of the decay of the ν_H at small angles relative to the ν_H direction; for the $\nu_H \to e\mu\nu$ decays, the topology has one such shower and a muon track; for the deep inelastic scattering processes $\nu_\mu N \to \nu_H X_1$ with subsequent decay $\nu_H \to \mu X_2$ the topology contains two showers separated by a space between the point of formation of the first shower, X_1, and the point of formation of the second shower, after the ν_H decay, in which a μ-meson track arises as well as the shower; for the $\nu_H \to e^- \pi^+$ decays the topology has a shower and a track of a π^+ meson with its subsequent decay.

As we have already noted, the heavy neutrinos ν_H can arise from decays of π or K mesons. A general theory of weak leptonic and semileptonic decays, including the possible existence of massive neutrinos and lepton mixtures, was given in Ref. 46. In the case of π- or K-meson decays, the boundary of the investigated region depends on the parameters of the experiment as follows:

$$|U_{lH} U_{l'H}| \geqslant f(m_{\nu_H}) \left[\frac{E_p}{\ln E_p N_p L}\right]^{1/2}.$$

It can be seen that the sensitivity increases with increasing N_p and L and decreases with increasing E_p. As a result the UNK can give only a moderate extension of the region, for example, as shown in Fig. 21 (for $L \simeq 300$ m and exposure of 100 days).

For comparison the broken curve in the same figure gives bounds on the values of the mixing matrix elements $|U_e|^2$ and $|U_e I_\mu|$ or $|U_\mu|^2$ obtained in one of the recent PS-191 experiments.[47] A review of data on the mixing matrix elements and references to earlier experiments on the same subject are given in Ref. 48. In contrast to this, for ν_H production in ν_μ and ν_e beams there is compensation of the factor E_p from the production and decay of the ν_H, and as a result we obtain

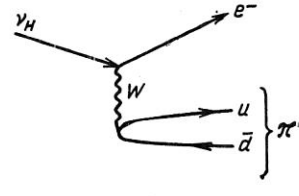

FIG. 19. Diagram of the process $\nu_H \to e^- \pi^+$.

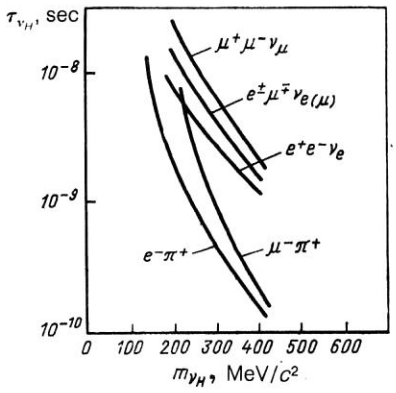

FIG. 20. Lifetimes of ν_H for different decay channels.[45]

$$|U_{lH}U_{l'H}| \geqslant f(m_{\nu_H})\left[\frac{1}{\ln E_p N_p L}\right]^{1/2}.$$

Therefore, the possibility of having large E_p, N_p, and L at the UNK can be used to extend significantly the investigated region, as is shown, for example, in Fig. 22 ($L/L_0 = 10$, $N_p/N_{p_0} = 10$, $E_p = 3$ TeV, $E_{p_0} = 400$ GeV).

Problems in the search for heavy neutrinos have been discussed in detail at recent working symposia and conferences.[51-53] The possible existence of a stable massive neutrino with vanishingly small electric charge ($\lesssim 10^{-20}$) and an experiment to detect it was discussed in Ref. 54.

Searches for heavy leptons

At the present time we know of three charged leptons—the electron, the muon, and the τ meson—and two (out of three) of the neutrinos corresponding to them: ν_e and ν_μ. As yet there are no direct proofs of the existence of the third, the τ neutrino. The leptons and the corresponding neutrinos form three lepton generations, the universality of whose interaction we discussed earlier.

There are no arguments that prohibit the existence of a fourth and, possibly, higher generations of charged leptons. In principle, indirect restrictions on the number of lepton generations can be obtained from knowledge of the number N_ν of different neutrino species (neutrino count). The currently existing estimates of the number N_ν are close to the values 4 or 5—from theoretical analysis of cosmological data $N_\nu < 4.0$ (possibly 5 or 6).[55] From theoretical analysis[56] of world data on elementary-particle physics (ASP, MAC, CELLO) it follows that $N_\nu < 4.9$ (90% C.L.). However, these estimates are not sufficiently strict.

Many experimental and theoretical studies have been made of the hypothesis of the fourth or higher generations of charged and neutral leptons and the experimental search for them.

A model of the mixing of neutral heavy leptons N with ordinary neutrinos in the framework of charged and neutral currents was considered in Ref. 57.

In the standard model the charged and neutral currents have the form

$$J^\mu_{CC} = \bar{\nu}_e\gamma^\mu e + \bar{\nu}_\mu\gamma^\mu\mu + \bar{\nu}_\tau\gamma^\mu\tau;$$
$$J^\mu_{NC} = \bar{\nu}_e\gamma^\mu\nu_e + \bar{\nu}_\mu\gamma^\mu\nu_\mu + \bar{\nu}_\tau\gamma^\mu\nu_\tau.$$

A simple generalization of these currents can be obtained by making the substitution

$$\nu_i \to N_i \approx \nu_i\left(1 - \sum_a \frac{|U_{ia}|^2}{2}\right) + \sum_a U_{ia}N_a.$$

Here, the sum over the index a is a sum over heavy leptons of species a. The weak eigenstate is now the state N_i; the mass eigenstates and ν_i (light) and N_a (heavy). The simplest case in which one light neutrino is mixed with one heavy neutrino was considered in the model of Ref. 57. In Fig. 23 we consider typical decay schemes of the heavy leptons. If the heavy lepton masses $1 \leqslant M_{Ni} \leqslant 2$ GeV/c^2, one can expect a decay of the type of hadronic final states (in accordance with the type of τ decays):

$$N \to l^-\pi^+;$$
$$\to l^-\pi^+\pi^0;$$
$$\to l^-\pi^+\pi^-\pi^+,$$

etc., where l^- is any negatively charged lepton. For heavier leptons, the final state will consist of a large number of different channels, and it will be more difficult to reconstruct.

The possibilities for looking for heavy leptons in the UNK neutrino beams are very limited. As we have already said, they can be seen only in interactions of neutrinos with heavy nuclei. Neutral leptons can be formed in these reactions through neutral currents and detected either near the production point, or, through the secondary vertices, after traversing a certain distance. In all cases it is necessary to look for unusual energy distributions of the leptons. The heavy quarks b and c produced in the neutrino beams can also decay semileptonically through the charged weak current into a neutral heavy lepton. In this case too it is necessary to seek second vertices in order to detect heavy leptons

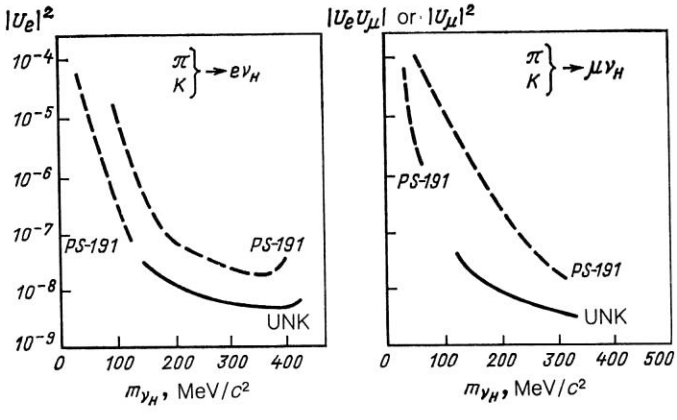

FIG. 21. Mixing matrix elements as functions of the mass of the heavy neutrino m_{ν_H}. The broken curves are the data of Ref. 47.

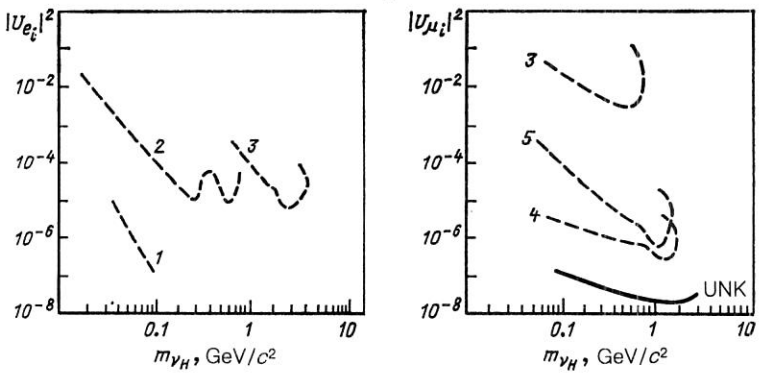

FIG. 22. Mixing matrix elements as functions of the mass m_{ν_H} of the heavy neutrino: 1) limits obtained by the CHARM collaboration[49] under the assumption of the decay chain $F \to \tau\nu_H$, $\tau \to \nu_\tau X$; 2) limits obtained by the CHARM collaboration[49] in a wide neutron beam; 3) limits obtained by the CHARM collaborations;[38] 4) in a beam-dump experiment (the same collaboration); 5) limits obtained by the BEBC collaboration in a beam-dump experiment.[50]

with their unusual energy balance. Similarly, heavy leptons can be sought in decays of ordinary or heavier (additional) W and Z bosons, whose decay signature will be similar to that of the decays $W \to l\nu$ and $Z^0 \to \nu\bar{\nu}$ with an additional secondary vertex. Experiments of beam-dump or νN-scattering type, in which all the considered cases in which heavy leptons can be manifested arise, can be a source of heavy leptons.

Serious difficulties in the search for heavy leptons are associated with our ignorance of the mass of the corresponding heavy neutrino accompanying the production or decay of the heavy lepton.[58]

The simplest way of detecting the heavy leptons $L_0^{\pm}$ is to observe their decays, for example,

$L^0 \to e^+e^-\nu_e$, $e^+\mu^-\nu_e$, $\mu^+e^-\nu_\mu$, $\mu^+\mu^-\nu_\mu$,

$L^- \to e^-X$, μ^-X, $\mu^-e^+e^-$, $\mu^-\mu^+\mu^-$.

The total decay width Γ of a sequential charged lepton is expressed by

$$\Gamma = \frac{Q_F^2 m_L^5}{192\pi^3}\left[3 + 6\left(1 + \frac{\alpha_s}{\pi}\right)\right],$$

where the first term in the square brackets corresponds to the decays $L \to \nu_L e\bar{\nu}_e, \nu_L\mu\bar{\nu}_\mu, \nu_L\tau\nu_\tau$, and the second to hadronic decays in accordance with the schemes $L \to \nu_L (u\bar{d}, c\bar{s})$. For $m_L = 40$ GeV/c^2, the expression for Γ leads to the value $\tau_L \approx 10^{-19}$ sec, which is much too small to lead to a significant track length.[59] A fairly complicated analysis of events involving one jet and missing energy led the authors of the UAI collaboration[60] to conclude that the heavy lepton has a mass $m_L > 41$ GeV/c^2. The background from decays of the t quark was not included. Inclusion of this background would raise the limits on the mass of the heavy lepton.

Investigations showed that with increasing mass of the heavy lepton the fraction of topological events with two jets and missing energy increases.[61] At the UNK energies the cross section for the production of heavy leptons is expected to increase, both for neutrino interactions and for hadronic interactions, in which heavy leptons may appear when K mesons decay:

$$p + A \to K^+ + X, \quad K^+ \to e^+L^0$$

or when charmed particles decay:

$$D \to eL, \ \mu L \ \ldots$$

By increasing the statistics of the single- and two-jet events with missing energy, one can hope to increase by 2–3 times the limit on the mass of the heavy leptons. As regards the background from the decay of the charmed and other heavy quarks, knowledge of the neutrino energies in narrow-spectrum beams and, especially, beams of tagged neutrinos will permit a significant suppression of the background (to the level 10^{-2}–10^{-4}), since these processes are associated with a hadronic and not leptonic vertex and typically have a small missing energy.

Higgs bosons

In the minimal standard model that we consider, with one Higgs doublet, there is one neutral Higgs meson H^0 with a well-defined Yukawa coupling constant:[2)] with the quarks,

$$g_{Hq\bar{q}} = \frac{em_f}{2(1-R^{1/2})M_W} = \frac{gm_f}{2M_W};$$

with the W bosons,

$$g_{HWW} = \frac{eM_W}{(1-R^{1/2})} = gM_W;$$

with the Z bosons,

$$g_{HZZ} = \frac{eM_Z}{2(1-R)^{1/2}} = \frac{gM_Z}{2},$$

where g is related to the Fermi constant G_F by $g^2/8M_W^2 = G_F/2$. It can be seen that the coupling constant increases with increasing mass of the particles that interact with the Higgs field, and as a result the Higgs boson is more likely to decay into heavier particles.

Below the WW threshold, but above the threshold for $c\bar{c}$ pair production, the decay of the H^0 boson in quark and lepton pairs has width[62]

$$\Gamma(H^0 \to f\bar{f}) = \frac{G_F m_f^2 m_H}{4\sqrt{2}}\beta_{f\bar{f}}^3,$$

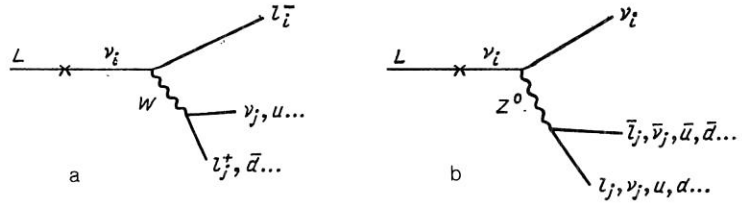

FIG. 23. Typical decay schemes of the neutral heavy lepton through the charged-current channel (a) and through the neutral-current channel (b) [$l = (e,\mu,\tau)$].

where $\xi = 3$ for quarks and $\xi = 1$ for leptons, and β_f is the velocity of the quark or lepton f in the rest frame of the H^0 boson. Thus, we have the ratio

$$\frac{\Gamma(H^0 \to ee)}{\Gamma(H^0 \to \mu\mu)} = \frac{m_e^2}{m_\mu^2},$$

$$\frac{\Gamma(H^0 \to ee)}{\Gamma(H^0 \to cc)} = \frac{m_e^2}{3m_c^2}.$$

If the mass of the H^0 is the interval $11\ \text{GeV}/c^2 < M_{H^0} < 2m_b$, the ratios of the decay probabilities will satisfy

$$\text{BR}(H \to e^+e^- : \mu^+\mu^- : \tau^+\tau^- : c\bar{c} : b\bar{b})$$

$$1 : \frac{m_\mu^2}{m_e^2} : \frac{m_\tau^2}{m_e^2} : \frac{3m_c^2}{m_e^2} : \frac{3m_b^2}{m_e^2}.$$

An estimate of the mass of the Higgs boson can be obtained from the radiative corrections calculated in the framework of the standard model. They also depend on the mass of the t quark. For $m_t = 45\ \text{GeV}/c^2$, analysis of the experimental data has yielded[63] the value $m_{H^0} \geqslant 100\ \text{GeV}/c^2$.[3)]

Estimates of the possibility of detecting Higgs bosons in the decays $\eta' \to \eta + H$ and $\psi' \to J/\psi + H$ lead to the conclusion that the present experimental data are not sufficiently sensitive to hope for positive results. With regard to searches for Higgs bosons in flavor-changing neutral currents, several theoretical calculations of the $s \to d + H$ and $b \to s + H$ processes do not agree with each other, and more accurate calculations are needed.[59] However, in this case too the fractions of $K^+ \to \pi^+ H$ and $B \to K + H$ decays will probably be below the sensitivity of modern experiments.

Searches for neutral bosons H^0 in decays of B mesons ($B \to H^0 K, H^0 K^*$) led to the conclusion that (for $m_t > 47\ \text{GeV}/c^2$) mass values

$$0.3 < m_{H^0} < 3.0\ \text{GeV}/c^2 \text{ and } 3.2 < m_{H^0} < 3.6\ \text{GeV}/c^2$$

can be excluded.[64,65]

In the standard model the mass of the Higgs boson is not determined; its limits; obtained in the framework of perturbation theory, are very wide:[66]

$$5\ \text{GeV}/c^2 \leqslant m_H \leqslant 1\ \text{TeV}/c^2.$$

The minimal supersymmetric extension of the standard model based on $N = 1$ supergravity theory imposes a rigorous upper bound on the mass of the light neutral Higgs boson—it must be less than the mass of the Z boson.[67] Restrictions on the masses of charged Higgs bosons and their coupling constants have been obtained in models with two Higgs doublets.[68] To analyze the B^0–$\bar{B}^0$ mixing processes, the authors selected the following Lagrangian of the interaction of the charged bosons with the quarks:

$$L_{\text{int}} = \frac{g}{2\sqrt{2}M_W} \chi^+ \bar{u} \times \left[\frac{\xi}{\eta} M_u K (1-\gamma_5) + \frac{\eta}{\xi} K M_d (1+\gamma_5)\right] d_x$$

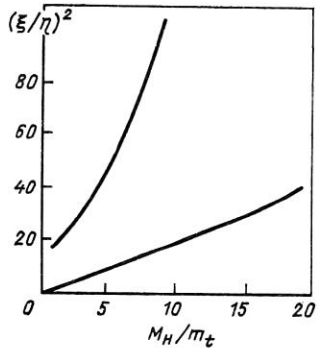

FIG. 25. Ranges of variation of the parameter $(\xi/\eta)^2$ as a function of the mass ratio M_H/m_t. the upper curve is the "pessimistic" estimate of the dependence, and the lower curve the "optimistic" estimate.[68]

where χ^+, $\bar{u}$, and d are the wave functions of the Higgs boson and the u and d quarks, respectively; K are the Kobayashi–Maskawa matrices; M_u and M_d are diagonal mass matrices for the charged quarks u and d with charges $+2/3$ and $-1/3$, respectively; the ξ and η are the vacuum expectation values for the unmixed Higgs fields associated with the quarks with charges $+2/3$ and $-1/3$, respectively. Examples of diagrams of "box" type that contribute to the B^0–$\bar{B}^0$ mixing are given in Fig. 24. It follows from the Lagrangian L_{int} that the interaction of the Higgs bosons with the quarks is proportional (or inversely proportional) to the factor ξ/η. The authors of Ref. 68 obtained an explicit dependence of the parameter ξ/η on the mass ratio m_H/m_t of the Higgs boson H and the t quark. The "pessimistic" (upper curve) and "optimistic" (lower curve) dependences of the parameter ξ/η on m_H/m_t are given in Fig. 25. The ratio ξ/η can be determined independently from other phenomena (for example, from the K_S–K_L mass difference). If the ratio ξ/η can be determined independently, then the values of the masses m_H and m_t will be determined within the limits shown in Fig. 25. The currently existing restrictions on the values of the parameter ξ/η lie in the range 5–10 units, and this leads to possible values $m_H \lesssim 0.5\ \text{TeV}/c^2$.

In the supersymmetric version of the extension of the standard model there are at least two Higgs doublets, these containing three neutral and two charged mesons (H_W^+ and $H_{\bar{W}}$ (see Table II). Charged bosons can be produced in the $e^+e^- \to H^+H^-$ reaction. Their preferred decay schemes are $H^\pm \to \tau\nu_\tau$, cs, or cb. Recent data obtained by the CELLO[69] and JADE[70] collaborations rule out masses of the charged Higgs bosons in the region from 3.5 to 19 Gev/c^2 (irrespective of the decay schemes).

For large masses of the neutral Higgs bosons, one could also consider decay schemes like $H^0 \to W^+W^-$, $H^0 \to Z^0Z^0$. However, even in $p\bar{p}$ collisions the cross section for production of the heavy Higgs bosons is very small.[71] The fraction of $H^0 \to W^+W^-$ decays is estimated at $\leqslant 2 \times 10^{-5}$. Therefore, neither for the existing CERN collider nor for the

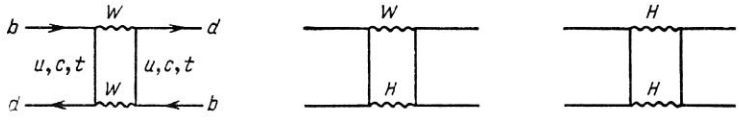

FIG. 24. Diagrams of "box" type that contribute to the B^0–$\bar{B}^0$ mixing in the model with two Higgs doublets; H is the charged Higgs boson.

future collider (ACOL) can one expect reliable statistics for which one could hope to detect the H^0 boson from decays into $W^+ W^-$ or ZZ.[59]

The search for heavy charged and neutral Higgs bosons in the UNK neutrino beam also has few prospects. Possible decay schemes of the H^0 bosons are shown in Fig. 12 and 13b. The cross sections for production of the bosons in these schemes will be smaller by a factor $(g/M_W)^2 \sim G_F$ than the cross sections for deep inelastic scattering.

Multilepton events

For a number of years the experimental, "well"-established fact that dileptons of the same sign are produced in neutrino interactions (at the level 10^{-3} of the production of single muons) has not found an explanation in the framework of the standard model. This fact cannot be explained by a contribution of $c\bar{c}$ pair production through a gluon or photon. In this case, the final state could have three muons, one of which, say, is not detected by the detector. Then the number of muon pairs of the same sign is appreciably less than the number of pairs detected in the experiments:[72]

$$\frac{\sigma_\nu(\mu^-\mu^-)}{\sigma_\nu(\mu^-)} \sim 5\cdot 10^{-5};$$

$$\frac{\sigma_{\bar{\nu}}(\mu^+\mu^+)}{\sigma_{\bar{\nu}}(\mu^+)} \sim 2.4\cdot 10^{-5}.$$

The effect also cannot be explained by the production of heavier quarks, for example, the cascade

$$\begin{array}{l} \bar{\nu}_\mu + u \to \mu^+ + b \\ \qquad\qquad\quad \hookrightarrow c + X \\ \qquad\qquad\qquad \hookrightarrow s + \mu^+ + \nu_\mu \end{array}$$

gives only about 10% of the total number of $\mu^+\mu^+$ pairs. Recent measurements by means of the CCFR detector at the Tevatron (Fermilab) at energy 800 GeV have apparently eliminated this difficulty.[73] This experiment was performed in the new energy region above 300 GeV. Events containing dimuons of the same sign with momentum greater than 9 GeV/c were selected. In the neutrino beam 102 ± 11.3 candidates were chosen (including a background of 89 ± 12.0 events), and in the antineutrino beam 15 ± 3.9 candidates were found (in this case the background was 9.9 ± 1.5 events). Thus, the production of dimuons of the same sign can be explained by the background.

The production of dileptons of opposite signs can be explained through the production and decay of charm:

$$\begin{array}{l} \nu_\mu N \to \mu^- + c + X \\ \qquad\qquad\quad \hookrightarrow \mu^+ + \nu_\mu + X'. \end{array}$$

Other mechanisms associated with a lepton vertex (for example, production of a heavy lepton L with subsequent decay $L \to \mu^+\mu^-\nu_\mu$) are incapable of explaining the observed angular and energy distributions of the muons, in particular, the presence of a leading μ meson.

The experiments have also revealed more complicated events containing three or four muons in the final state. Investigations have shown[74] that these events can be explained without recourse to the exotic schemes that have been proposed in a number of studies involving Higgs mesons, b and t quarks, or heavy leptons; one can describe these processes by means of radiative ($\simeq 1/3$) and hadronic ($\simeq 2/3$) production mechanisms with $\gamma \to \mu^+\mu^-$ and $\gamma, g \to c\bar{c}$ vertices. Experimentally, $\sigma(3\mu)/\sigma(\mu) \simeq 3\times 10^{-5}$ and $\sigma(4\mu)/\sigma(\mu) \sim 10^{-6}$.

The study of coherent neutrino-induced production of lepton pairs in the Coulomb field of a nucleus, $\nu A \to \nu e^+ e^- A$, which we considered in the first part of the review, is of great interest. This process is one of the (few) sources of information about the interference of the neutral and charged currents; however, the experimental separation of coherent events in this reaction is difficult, and at the present time there are no reliable data.[76]

The study of multilepton events, in the first place the production of lepton pairs of the same sign, is one of the most interesting problems in which experiments at the UNK could play an important part. This problem is already fairly complicated because the signal is $\lesssim 10^{-3}$ of the total cross section, so that in order to obtain $\simeq 10^3$ pairs of one sign it is necessary to have $\simeq 10^6$ charged-current events. However, as we have already noted in the Introduction, the achievement of such statistics at the UNK will not present problems. To elucidate the nature of the phenomena, it is necessary to make a detailed measurement of the dependence on x, y, $\sqrt{s}$, and p_T (for the second lepton relative to the produced hadrons) and a detailed test of the universality of the production of the various pairs ($\mu^+\mu^+$, $\mu^-\mu^-$, $e^\pm e^\pm$, $e^\pm\mu^\pm$). It is very desirable to see the vertex (to establish whether any long-lived particle is produced) and study the hadronic accompaniment of the pairs.

Additional gauge bosons

The energy of the UNK neutrino beams, even for interaction with heavy nuclei, will probably still be below the threshold for direct production of additional gauge bosons (if their masses are $\gtrsim 500\,\mathrm{GeV}/c^2$). Here, we discuss a number of indirect manifestations of these bosons.

Additional gauge bosons can be introduced in a number of ways. We briefly consider some of them. The first is to extend the standard model by including right currents—the gauge group is extended to $SU(2)_L \otimes SU(2)_R \otimes U(1)$.[76] In this case the well-known $W^\pm$ and Z^0 bosons are augmented by two charged bosons $W_R'^{\pm}$ and the one neutral boson Z'^0. If it is assumed that the constants of their coupling to the leptons are the same as for the ordinary W and Z bosons, restrictions on the masses of the additional charged gauge bosons can be obtained, for example, from the decay of μ mesons.[77] Physical W_1 and W_2 bosons are introduced in accordance with the standard mixing scheme:

$$W_1 = W_L \cos\xi - W_R \sin\xi;$$
$$W_2 = W_L \sin\xi + W_R \cos\xi.$$

The decay of the μ meson is then calculated with allowance for the contributions of the left and right currents.

The spectrum of positrons in the decay of polarized μ^+ mesons was measured in Ref. 78. Comparison of the experimental data with the theoretically calculated shape of the spectrum yielded the following bounds: For an infinitely heavy W_R boson the mixing angle must be $|\xi| < 0.045$; for any mixing angle ξ we must have $M_{W_R} > 380\,\mathrm{GeV}/c^2$; and for zero mixing angle $M_{W_R} > 450\,\mathrm{GeV}/c^2$ (the contribution of a possible right neutrino was ignored). Various schemes for including additional gauge bosons were considered in

Ref. 79: a) right W_R bosons; b) additional Z bosons in $SO(10)$ symmetry (denoted by Z_χ); c) a third z boson in E_6 symmetry (denoted by Z_ψ); d) neutral bosons with Yang–Mills couplings. Special ways of introducing a neutral boson into flavor-diagonal neutral currents were considered in Ref. 80: 1) the case of inclusion of Higgs bosons (all Higgs fields with nonzero vacuum expectation value, either doublets or singlets with respect to the weak $SU(2)$ group); 2) the case without any assumptions about the Higgs sector of the theory. The complete analysis of the experimental data on weak neutral currents[63] included a search for possible manifestations of additional neutral bosons. The following lower limits on the masses of the Z bosons were obtained at the 90% confidence level: $M_{Z_R} > 325$ and 343 GeV/c^2, $M_{Z_\chi} > 273$ and 249 GeV/c^2, and $M_{Z_\psi} > 154$ and 151 GeV/c^2, respectively, for the cases 1 and 2 mentioned above.[4)] At the UNK these limits could be shifted to 400–500 GeV/c^2.

Bednyakov and Kovalenko[81] calculated the contribution of the additional Z' boson to elastic νp scattering, to coherent neutrino production of π^0 mesons on nuclei, and to some diffraction processes in the framework of the E_6 superstring model. In their opinion, the relative contribution may reach an appreciable value and does not depend on the energy of the neutrino beams. In order to extract information about the contribution of the additional Z' boson, the cross sections of the processes in the UNK neutrino beams must be measured to a high accuracy (1–3%).

In conclusion we estimate the possibilities for producing additional bosons in pp or $p\bar{p}$ colliders.[82] The criterion for discovery was taken to be the production of 1000 gauge bosons in the rapidity range $|y| < 1.5$. For the $p\bar{p}$ collider with energy 40 TeV in the center-of-mass system integrated luminosities of 10^{38}, 10^{39}, and 10^{40} cm^{-2} are required to detect heavy W bosons with masses 2.4, 4.7, and 8.0 TeV/c^2, respectively. For the same luminosities the maximum masses of the additional Z' bosons take the values 1.9, 3.8, and 7.1 TeV/c^2, respectively.

Searches for supersymmetric particles

The most direct way of testing supersymmetry is to observe the production and decay of supersymmetric particles. Reactions in which they can be produced in the UNK neutrino beams are represented in the diagrams of Figs. 12–15. Other reactions, not shown in these diagrams, are also possible. We do not give a complete list of them in view of the very restricted possibilities for observing events of production of these particles in the UNK neutrino beams (only in interactions with heavy nuclei). As follows from the hypothesis of conservation of the R parity (see above), the final state must necessarily contain an even number of supersymmetric particles (2, 4, or more). They can decay, producing jets and new supersymmetric particles. If the decay of these particles proceeds to the end, the lightest supersymmetric particle must be left at the end, and it will carry away part of the energy and momentum. Thus, the universal topology of events with the production (and subsequent decay) of supersymmetric particles corresponds to events with jets and missing energy and momentum.

We mention some qualitative features of searches for supersymmetric particles. The scheme for direct production of a $\tilde{Z}^0\tilde{W}^-$ pair in a UNK neutrino beam is shown in Fig. 13a (it will not be observed in the UNK). If $M_{\tilde{l}} < M_{\tilde{W}^\pm, \tilde{Z}}$, one can expect decays of the type

$$\tilde{W}^\pm \to \tilde{l}^\pm \nu, \ \tilde{q}\bar{q}, \ \tilde{\tilde{q}}q \ , \ \text{etc.},$$

$$\tilde{Z} \to \tilde{l}l, \ \tilde{\nu}\nu, \ \tilde{q}\bar{q} \ , \ \text{etc.}$$

They are all events of decays with missing energy and the presence of one, two, three, or even four jets. Searches for winos (and also $\tilde{e}$, $\tilde{q}$, and $\tilde{g}$) have been made at CERN using the $p\bar{p}$ collider.[83]

Direct production of supersymmetric leptons in UNK neutrino beam is possible on heavy targets if the masses of the supersymmetric leptons are less than 250 GeV/c^2. It is difficult to estimate their production cross section, but, as follows from scaling arguments, it will be less than the cross section for deep inelastic scattering by at least a factor $(M_W/M_q)^2$.

The $\tilde{\nu} \to \nu\tilde{\gamma}$ decay is unobservable and leads to events with missing energy and momentum. The $\tilde{l}^\pm \to l^\pm \tilde{\gamma}$ decay is expected to be the main decay.

Schemes of direct production of supersymmetric quarks, photinos, and gluinos in the neutron beams of the UNK (provided the masses of the supersymmetric particles are less than 250 GeV/c^2) are shown in the diagrams (see Figs. 13b and 15). The search for these particles includes a wide variety of schemes of analysis. If $M_{\tilde{q}} > M_{\tilde{g}}$, then the $\tilde{q} \to q\tilde{g}$ decay is expected to be dominant. If the $\tilde{q}$ mass is greater than the wino or zino masses, then the decays $\tilde{q} \to q\tilde{W}$ and $\tilde{q} \to q\tilde{Z}$ are possible. In addition, $\tilde{q} \to q\tilde{\gamma}$ decays are possible. If $M_{\tilde{q}} < M_{\tilde{g}}$, then one can expect the decay $\tilde{g} \to q\bar{q}\tilde{\gamma}$ to be dominant. For $M_{\tilde{\gamma}} > M_H$ the decay $\tilde{\gamma} \to \gamma\tilde{H}$ is possible.

Obviously, all these and other possible decay schemes must be included in a program of analysis of events in a search for supersymmetric particles. Searches for supersymmetric leptons, quarks, photinos, and gluinos have been made at CERN by the UA2 (Ref. 83) and UA1 (Ref. 84) collaborations.

Searches for supersymmetric particles have also been made with the detectors ASP (Ref. 85), MAC (Ref. 86), and MARK II (Ref. 87) at the e^+e^- collider PEP (SLAC) and by the collaborations CELLO (Ref. 32), JADE (Ref. 88), MARKJ (Ref. 89), the TASSO (Ref. 90) at the e^+e^- collider PETRA.

Neutrino oscillations and masses

One of the most interesting phenomena that occur in the presence of mixing is neutrino oscillations, i.e., the periodic (complete or partial) transformation of neutrinos of one species into another.[91–93] The oscillations are the most sensitive means for determining possible small masses and mixing angles of neutrinos. The existing experiments give the following restrictions on m_ν. From tritium β decay, $m_{\nu_e} = 26 \pm 6$ eV/c^2 (IHEP), $m_{\nu_e} < 27$ eV/c^2 (LANL, 1987), $m_{\nu_e} < 28$ eV/c^2 (INS, 1988), $m_{\nu_e} < 18$ eV/c^2 (SIN, 1986); for ν_μ and ν_τ: $m_{\nu_\mu} < 285$ keV/c^2, $m_{\nu_\tau} < 35$ MeV/c^2 (all at 95% confidence level).[94] Double β decay gives $m_{\nu_e} < 1$–2 eV/c^2, but the results are model-dependent. The spreading of the neutrino pulse from the recent supernova SN 1987A can be interpreted as an indication of $m_{\nu_e} \sim 10$–15 eV/c^2.[94] Astrophysical estimates limit the sum of the masses of all neutrino species to 50–100 eV/c^2. However, the cosmologi-

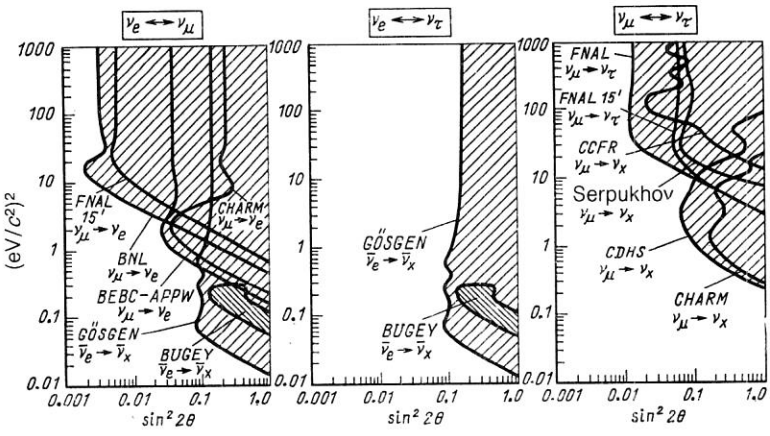

FIG. 26. Range of Δm^2 and $\sin^2 2\theta$ values ruled out by modern experimental data (hatched).

cal arguments do not rule out very heavy neutrinos with masses greater than a few giga-electron-volts. Finally, the existing data on searches for oscillations rule out the region of $\Delta m_{ij}^2 = |m_i^2 - m_j^2|$ and $\sin^2 2\theta_{ij}$ shown in Fig. 26.

As we have already said, at the present time there are no sufficiently reliable theoretical predictions for the values of m_{ν_i} and θ_{ij}. This means that searches for possible manifestations of neutrino masses and mixing must be made in the entire range of these parameters accessible to measurement. Nevertheless, it is expedient to bear in mind the predictions of some of the popular models. For example, in various grand-unification scenarios a hierarchy of neutrino masses is predicted. Small neutrino masses are ensured by the seesaw mechanism[33] without the introduction of any new small mass scale. It is assumed that as a result of symmetry breaking the right neutrinos acquire Majorana masses of the order of the grand-unification scale, whereas the Dirac mass terms acquire the ordinary mass scale of the quarks and leptons. As a result the mass eigenstates of the neutrinos ν_i (small mixing angles $\nu_1 \simeq \nu_e$, $\nu_2 \simeq \nu_\mu$, $\nu_3 \simeq \nu_\tau$) acquire a "direct (linear or quadratic) horizontal hierarchy" of the masses:

$$m_{\nu_1} : m_{\nu_2} : m_{\nu_3} \sim m_e : m_\mu : m_\tau \sim \sim 10^{-3} : 10^{-1} : 1 \text{ (or } \sim m_e^2 : m_\mu^2 : m_\tau^2). \quad (1)$$

Another interesting possibility is associated with the idea of local $SU(3)_H$ chiral symmetry,[95,96] for which the families (u,d,e,ν_e), (c,s,μ,ν_μ), and (t,b,τ,ν_τ) are combined in such a way that the left components of the quarks and leptons are in $SU(3)_H$ triplets, and the right components in $SU(3)_H$ antitriplets. A consequence of this is a "reverse horizontal hierarchy":

$$m_{\nu_1} : m_{\nu_2} : m_{\nu_3} \sim m_e^{-1} : m_\mu^{-1} : m_\tau^{-1} \sim 1 : 10^{-2} : 10^{-3}. \quad (2)$$

As was noted in Ref. 97, a large ν_e mass is compatible with the cosmological restrictions on the ν masses only for the reverse hierarchy. In such models the absolute mass scale is noted determined. If nominally we take ~ 1 eV as the mass of the heaviest neutrino, then From Eqs. (1) and (2) we obtain

$$m_{\nu_e} \sim 10^{-3} \text{ eV}/c^2; \; m_{\nu_\mu} \sim 10^{-1} \text{ eV}/c^2;$$

$$m_{\nu_\tau} \sim 1 \text{ eV}/c^2 \text{ (direct hierarchy);}$$

$$\Delta m_{13}^2 \sim \Delta m_{23}^2 \sim 1 \text{ eV}^2/c^4; \; \Delta m_{12}^2 \sim 10^{-2} \text{eV}^2/c^4;$$

$$m_{\nu_e} \sim 1 \text{ eV}/c^2; \; m_{\nu_\mu} \sim 10^{-2} \text{ eV}/c^2;$$

$$m_{\nu_\tau} \sim 10^{-3} \text{ eV}/c^2 \text{ (reverse hierarchy);}$$

$$\Delta m_{12}^2 \sim \Delta m_{13}^2 \sim 1 \text{ eV}^2/c^4; \; \Delta m_{23}^2 \sim 10^{-4} \text{ eV}^2/c^4.$$

Another possibility is to assume that the solar-neutrino problem is solved by the Mikheev–Smirnov–Wolfenstein mechanism.[98,99] Then $\Delta m_{12}^2 \sim 10^{-7}$–$10^{-4}$ eV$^2/c^4$, whence $\Delta m_{13}^2 \sim \Delta m_{23}^2 \sim 10^{-5}$–$10^{-2}$ eV$^2/c^4$ for the direct hierarchy and $\Delta m_{13}^2 \sim \Delta m_{12}^2$, $\Delta m_{23}^2 \sim 10^{-11}$–$10^{-8}$ eV$^2/c^4$ for the reverse hierarchy.

With regard to the neutrino mixing angles, it can be expected they do not differ very strongly from the quark mixing angles. In the various schemes they typically have an order of magnitude determined by the mass ratio of the corresponding quarks or leptons:

$$\sin \theta_{ll'} \sim \sqrt{m_l/m_{l'}}.$$

Then

$$\sin^2 \theta_{e\mu} \sim 10^{-2}, \; \sin^2 \theta_{e\tau} \sim 10^{-3}, \; \sin^2 \theta_{\mu\tau} \sim 10^{-1}. \quad (3)$$

Using these values, we can estimate the expected amplitudes and lengths of the oscillations in the vacuum:[97]

$$P_{ab} = P_{ab}^0 \sin^2(\pi L/L_{ab}); \; P_{ab}^0 = \sin^2 2\theta_{ab}; \quad L_{ab} = 4\pi E_\nu/\Delta m_{ab}^2 \simeq 2.5 E_\nu/\Delta m_{ab}^2, \quad (4)$$

where E_ν is measured in GeV, Δm_{ab} in eV$/c^2$, and L in km. It follows from (4) that

$$P_{\mu\tau}^0 \sim 10^{-1}, \; P_{e\mu}^0 \sim 10^{-2}, \; P_{e\tau}^0 \sim 10^{-3}.$$

Assuming again that the mass of the heaviest neutrino is ~ 1 eV$/c^2$, and bearing in mind that the range of UNK energies is $E_\nu \sim 10^1$–10^3 GeV, we obtain

$$L_{e\tau} \sim L_{\mu\tau} \sim 25 - 2500 \text{ km};$$

$$L_{e\mu} \sim 2.5 \cdot 10^3 - 2.5 \cdot 10^5 \text{ km (direct hierarchy);}$$

$$L_{e\mu} \sim L_{e\tau} \sim 25 - 2500 \text{ km};$$

$$L_{\mu\tau} \sim 2.5 \cdot 10^3 - 2.5 \cdot 10^5 \text{ km (reverse hierarchy).}$$

A very important advantage of accelerator experiments in the search for oscillations (particularly using the UNK beams) is the possibility of achieving a very high accuracy of the measurements and, therefore, determining very small mixing angles. Thus, in the inclusive $\nu_\mu \to \nu_X$ ($\nu_e \to \nu_X$) experiment one can obtain a restriction (statistical accuracy only!) on $\sin 2\theta$ at the level $\sim 5 \times 10^{-5}$ (3.5×10^{-4}); this is two to three orders of magnitude better than the existing bounds and is beyond the scope of other methods.

Of particular interest is the exclusive arrangement in beams of tagged neutrinos, which ensure a high systematic accuracy by virtue of the monitoring and purity of the beam. This applies above all to searches for $\nu_e \to \nu_\mu$ transitions in a

ν_e beam. Although the ν_e beam will have less intensity than the ν_μ beam, this is compensated by the possibility of reliable detection of the final muon from the $\nu_e \to \nu_\mu$ and $\nu_\mu N \to \mu + X$ processes. The statistics in a detector of mass 500 ton will permit measurement of $\sin^2 2\theta$ at the level $\sim 2 \times 10^{-3}$. A further feature of tagged neutrinos is associated with the possibility of highly accurate measurement of E_ν and the interaction point ($\Delta L \sim 50$ m) and investigation of the oscillations directly with respect to the variable L/E (Ref. 100).

We now discuss the possibility of measuring the parameter Δm^2, which determines the oscillation length. For accelerator experiments, an increase in the sensitivity to Δm^2 requires an increase in the ratio L/E, i.e., removal of the detector to great distances. We shall discuss the unique possibilities of beams of "long-distance" UNK neutrinos in Sec. 3. As regards "laboratory" investigations, on a base of up to 50 km, which is permitted by the profile of the locality and the trajectory of the neutrino beam, they can surpass typical present-day accelerator experiments, which have $L/E \sim 0.025$–0.05 km/GeV, but are inferior to the best experiments, which have $L/E \sim 1$ km/GeV. Nevertheless, because of the high accuracy of the measurements they will make it possible to achieve a level of $\Delta m^2 \sim 0.05$ eV$/c^4$ (Ref. 101).

Since $\theta_{\mu\tau}$ is expected to be the largest mixing angle, one of the most interesting and promising tasks for the UNK may be the search for $\nu_\mu \to \nu_\tau$ oscillations.[101]

3. POSSIBLE INVESTIGATIONS WITH LONG-DISTANCE NEUTRINOS

Beams of long-distance neutrinos,[102] i.e., neutrinos detected at large distances from the UNK accelerator, give unique possibilities for investigations in both neutrino physics and "neutrino geophysics."[102–107]

Such investigations are distinguished from ordinary "laboratory" experiments by the great length of the base traversed by the neutrinos from the production point to the detector and by the large amount of matter in the path of the neutrinos. This makes it possible to enhance some aspects that under ordinary conditions are either not observed at all or are seen only very weakly. In contrast to measurements with neutrinos of atmospheric or cosmic origin, experiments with accelerator beams are characterized by well-controlled conditions (energy, intensity, time structure, beam direction). Here, we shall not discuss the problems associated with the formation and detection of long-distance neutrino beams. These questions have been fairly well considered in reviews.[102,105,106] We merely note that for a rough estimate of the possibility of detecting neutrinos at large distances from the accelerator one can use a simple relation that (under the assumption of ideal focusing) establishes a connection between the flux density dN_μ/ds of the equilibrium muons that accompany the ν_μ beam (on the beam axis), the proton energy E_p, the length l of the decay channel, the number N_p of protons in the pulse, and the distance L (Refs. 102 and 105):

$$\frac{dN_\mu}{ds} \simeq 2.4 \cdot 10^{-16} \frac{l N_p E_p^3}{L^2}, \qquad (5)$$

where l is measured in km, E_p in TeV, L in 10^3 km, and dN_μ/ds in m^{-2}.

Taking $N_p = 5 \times 10^{14}$ protons per accelerator pulse, $l = 1$ km, and $E_p = 3$ TeV, we obtain for the muon flux from the UNK at distance L

$$(dN_\mu/ds)_{\text{UNK}} \simeq 3/L^2.$$

More accurate estimates that take into account the real spectra will be given later.

With regard to the technical problems, the main ones are associated with ensuring deflection of the extracted proton beams relative to the plane of the equilibrium orbit (for example, for distances $L = 1000$, 1400, 2500, 4300, and 12 800 km the necessary deflection angles are, respectively, $\alpha \simeq 4.5$, 6.2, 11.3, 19.6, and 90°) and with the creation of a decay tunnel with a length from several hundred meters to several kilometers, oriented in the required direction.

Neutrino oscillations

One of the most important problems is to search for neutrino oscillations. Here, the use of beams of long-distance neutrinos is of interest for numerous reasons:

a) In inclusive ("leaving out") experiments with ν_μ beams ($\nu_\mu \to \nu_X$), or exclusive experiments, $\nu_e \to \nu_\mu$, the flux density of the equilibrium muons accompanying the ν_μ beam is, as can be seen from (5), proportional to the cube of the energy E of the neutrinos or of the primary protons and inversely proportional to the square of the distance L. This means that if the ν_μ are detected by the muons that they produce in the matter in front of the detector, then to investigate the oscillation effect (which depends on the ratio L/E) it is advantageous (for unchanged detector area) to take the detector to large distances, going over simultaneously to higher energies.[108] If the ratio L/E is kept constant, then, leaving the phase factor in (4) unchanged, we simultaneously increase the statistical reliability of the measurements through the extra power of E in (5) and, thus, raise the sensitivity of the experiment to the value of $\sin^2 2\theta$. Another possibility is to keep dN_μ/ds, i.e., the statistical reliability of the measurements, fixed and increase the sensitivity to Δm^2 by increasing the ratio L/E by $\sim\sqrt{E}$ times.

b) For large base lengths

$$L \gtrsim L_0 = 1/\sqrt{2}\, G N_e \simeq 3.5 \cdot 10^4/\rho$$

[G is the Fermi constant, N_e is the electron density, ρ is the matter density (g/cm^2), and L_0 is the Wolfenstein length (km)]. The influence that the matter of the earth has on the nature of the oscillations can become important.[98] By performing experiments with $L \gtrsim 1000$ km, one can study this interesting phenomenon, which in recent years has been widely discussed in the literature,[99] mainly in connection with the possible detection of neutrino fluxes from astrophysical sources (the sun, supernova explosions, etc.). Despite the undoubted advantages of such experiments that accrue above all from the great distances and matter densities, the astrophysical measurements are subject to great uncertainties that make their interpretation more difficult. In Refs. 98 and 109 attention was drawn to the possibility of investigating oscillations in the matter of the earth in experiments with accelerator neutrinos, which to a large degree are free of these shortcomings. Over global distances in the earth the effects can be appreciable,[109] since the Wolfenstein length L_0 for characteristic densities $\rho \sim 3$–10 g/cm^3 is

$\sim$12 000–3500 km, i.e., comparable with the diameter of the earth. This is a consequence of the fortuitous order-of-magnitude equality of two quantities that have different physical significances—the reciprocal Fermi constant $G^{-1} \simeq 2\times 10^{32}$ cm^{-2} and the number of electrons per unit area along the diameter of the earth.[109]

It is important to emphasize that for small mixing angles the amplitude of the oscillations in vacuum is small and may be insufficient for direct measurements. It is possible that only enhancement of the oscillations in matter (over large base lengths L) will permit their detection and study. In summary, experiments with long-distance neutrinos make it possible to advance into an uninvestigated region of values of the oscillation parameters Δm^2 and $\sin^2 2\theta$.

c) In experiments at large distances the possibility is opened up to detecting effects associated with the T (CP)-violating phase in the mixing matrix of the lepton sector.[93] In matter these effects can be enhanced by several times.[110,111]

d) Finally, measurement of the energy dependence of the probability of transitions due to neutrino oscillations can give important information about the structure of the earth and the profile of the matter density distribution.[109,112]

Oscillations in matter

As was first noted by Wolfenstein,[98] the nature of the oscillations is changed in a medium, owing to the difference between the interaction of ν_e and of ν_μ and ν_τ with the components of the medium (because of the contribution of the charged current to $\nu_e e \to \nu_e e$ scattering). In the case of a medium with constant density, $\rho = \bar{\rho}$, we have in place of (4)

$$P(\nu_l \to \nu_{l'}) = \frac{\sin^2 2\theta}{\omega^2} \sin^2 \omega\tau, \tag{6}$$

where

$$\omega = \left[1 - 2\cos 2\theta \frac{L_\nu}{L_0(\bar{\rho})} + \left(\frac{L_\nu}{L_0(\bar{\rho})}\right)^2\right]^{1/2}$$

and L_ν is the oscillation length in vacuum. As can be seen from (6), in matter with $\rho = \bar{\rho} = \text{const}$ the effective oscillation parameters in $\sin 2\theta_m = \sin 2\theta/\omega$ and $L_m = L_\nu/\omega$. If the resonance condition[99]

$$L_\nu/L_0 = \cos 2\theta \tag{7}$$

is satisfied, we have $\omega = \sin 2\theta$, and the oscillation amplitude becomes equal to unity for any angle θ.

The oscillations $\nu_l \to \nu_{l'}$ in a medium with variable density are described by the Schrödinger equation for the two-component amplitude $\psi = \begin{vmatrix} \nu_l \\ \nu_{l'} \end{vmatrix}$,[99]

$$i\frac{d\psi}{dt} = H\psi, \tag{8}$$

where

$$H = \pi \begin{pmatrix} \frac{\cos 2\theta}{L_\nu} - \frac{1}{L_0(t)} & -\frac{\sin 2\theta}{L_\nu} \\ -\frac{\sin 2\theta}{L_\nu} & -\frac{\cos 2\theta}{L_\nu} + \frac{1}{L_0(t)} \end{pmatrix};$$

and $t = x/c = x$. In practical applications it is convenient,[109] eliminating the component $|\nu_l\rangle$, to reduce (8) to a second-order equation for the amplitude $|\nu_{l'} \equiv \xi$:

$$\frac{d^2\xi}{dt^2} + f(t)\,\xi = 0;$$

$$f(t) = \pi^2 \left(\frac{1}{L_0^2(t)} - \frac{2\cos 2\theta}{L_\nu L_0(t)} + \frac{1}{L_\nu^2}\right) + i\pi \frac{d}{dt}\left(\frac{1}{L_0(t)}\right) \tag{9}$$

with initial conditions (for the original $\nu_{l'}$ beam)

$$\xi(0) = 0;\ d\xi(0)/dt = i\sin 2\theta. \tag{9'}$$

The solution of Eq. (9) gives $P_{\nu_l - \nu_{l'}}(t) = |\xi(t)|^2$. It is also important to emphasize that the sign of the $\bar{\nu}_l e$ scattering amplitude ($l = e, \mu, \tau$) is opposite to the sign of the $\nu_l e$ scattering amplitude, this corresponding to the substitution $L_0 \to -L_0$. This means that a resonance can arise either for ν or for $\bar{\nu}$, but not for both simultaneously. Thus, the observation of oscillations in matter makes it possible in principle to determine the sign of $L_\nu \sim (m_1^2 - m_2^2)^{-1}$ (Ref. 113).

Some estimates for the UNK beams

To illustrate the possibilities of investigating oscillations with beams of long-distance neutrinos from the UNK, we give some estimates[109] for oscillations in a system of two neutrinos for the following characteristic distances L: 1000 km (scale of distances over which the influence of the matter of the earth is small, and vacuum oscillations can be studied); 1400 km, the distance from the UNK (at Serpukhov) to the Baksan Neutrino Observatory, which could serve as the neutrino detector; 2500 km, the distance to the water basin near Naples, where an underwater detector could be situated (an idea of M. A. Markov); 4300 km, the distance to Lake Baikal, where an underwater Cherenkov detector of the Institute for Nuclear Research of the USSR Academy of Sciences is currently being equipped; and, finally, 12 800 km, the greatest distance within the terrestrial ball, at which the effect of the oscillations could reach a maximum. With regard to the beams, the following is assumed: a) the primary protons have energy 600 GeV (first step of the UNK) or 3000 GeV (second step of the UNK), intensity 6×10^{14} protons per pulse, and pulse repetition cycle of 2 min ($\sim 2\times 10^4$ pulses per month); b) the secondary mesons, the progenitors of the neutrinos, are either perfectly focused or not focussed at all (the estimates for real focusing lie between the limits for these cases); c) the initial neutrino beam contains ν_μ, and either ν_μ or ν_e are detected. The length of the decay channel is taken to be 500 m. The characteristic angular dimensions of the neutrino beam are $\alpha \sim 1/\langle\gamma_\pi\rangle$, giving $\sim 10^{-3}$ for $E_p = 600$ GeV and $\sim 2\times 10^{-4}$ for $E_p = 3000$ GeV. The corresponding radius of the neutrino "spot" at distance 1000 km is $\simeq 1$ km and 0.2 km, respectively.

It is known from seismological measurements[114] that the density $\rho(x)$ (and the related electron-number density N_e, which occurs in L_0) varies quite appreciably within the earth: from $\rho \sim 12$ g/cm^3 at the center of $\rho \sim 2.5$ g/cm^3 near the surface. At the core–mantle boundary at $x \simeq 3500$ km there is an abrupt jump in the density. Since L_0 is comparable with the distance over which significant changes in $N_e(x)$ occur, we cannot solve (9) using an approximation in which $N_e(x)$ is approximated either by a step or "adiabatically."[99] Therefore, to obtain a sufficiently accurate result one must find a numerical solution of the equation on a computer, including a model of the matter density distribution in the

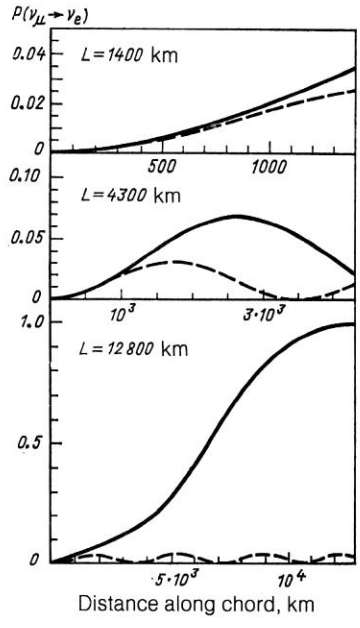

FIG. 27. Probability $P(\nu_\mu \to \nu_e)$ as a function of the distance along chords of different lengths; $\sin^2 2\theta = 0.03$, $\Delta m^2/E_\nu = 7.143\times10^{-4}$ eV^2/(GeV$\cdot c^4$).

earth currently adopted in geophysics.[114] The amount of mater on a path of the neutrino beam in the earth of length 1000, 1400, 2500, 4300, and 12 800 km is, respectively, 2.96×10^8, 4.13×10^8, 7.76×10^8, 1.45×10^9, and 1.04×10^{10} g/cm^2; for these values the neutrino absorption does not exceed tenths of a percent.[102]

In Table IV we give characteristics of $\nu_\mu N \to \mu^- + \ldots$ events, and also the fluxes of the neutrinos and equilibrium muons on the beam axis. We also give the number of events N_{ev} and the number of equilibrium muons N_μ per accelerator cycle for nominal detectors with mass $M = 10^6$ ton or muon detection area $S = 10^4$ m^2.

The results of numerical calculations of $P(\nu_\mu \to \nu_e)$ by means of Eq. (9) are shown in Figs. 27–30. Figure 27 shows the $\nu_\mu \to \nu_e$ transition probability as the neutrinos move along chords of different lengths. It can be seen that for $L = 1400$ km the oscillations are close to the vacuum values, whereas for $L = 4300$ and especially 12 800 km the influence of the matter of the earth is important. Moreover, for the chosen values of the parameters, $\Delta m^2/E_\nu \simeq 7.143\times10^{-4}$ eV^2/($c^4\cdot$GeV) and $\sin^2 2\theta = 0.03$, the amplitude of the oscillations over the earth's diameter is larger than the vacuum value by a factor of about 33 and reaches unity. This is a result of the resonance effect.[99] Note that in the earth the resonance condition

$$\frac{L_\nu}{L_0} \simeq \frac{E_\nu \rho}{1.4\cdot10^4 \Delta m^2} = \cos 2\theta \simeq 1$$

is satisfied in a wide range of values of Δm^2 and $\sin^2 2\theta$ that are allowed by present-day experimental data with allowance for the possibility of variation of the energy E_ν in the range $1 \lesssim E_\nu \lesssim 10^3$ GeV. If the resonance condition is to be satisfied at distance $\Delta x \approx L_{res}/2 = L_0/2 \tan 2\theta$ [and, accordingly, the probability $P(\nu_\mu \to \nu_e)$ is to be near unity], it is sufficient that over this distance the variation $\delta(L_\nu/L_0)$ due to the change in the density be less than the width of the resonance: $\delta(L_\nu/L_0) < \Delta(L_\nu/L_0) = \sin 2\theta$.[99] The most favorable conditions for resonance are realized in the core of the earth when the neutrinos move along its diameter. Here,

TABLE IV. Properties of $\nu_\mu N \to \mu^- + \ldots$ events and fluxes of neutrinos and equilibrium muons on the beam axis.

E_p, GeV	Distance L to detector, km	ν_μ flux		ν_μ events in volume of detector		Flux of equilibrium muons		N_{ev}	N_μ
		dN_ν/ds, proton^{-1}m^{-2}	$\langle E_\nu \rangle$, GeV	dN_c/dM, proton^{-1}ton^{-1}	$\langle E_\mu \rangle$, GeV	dN_μ/ds, proton^{-1}m^{-2}	$\langle E_\mu \rangle$, GeV		
600	1000	$2.0\cdot10^{-8}$ $2.7\cdot10^{-10}$	22	$1.9\cdot10^{-19}$ $5.0\cdot10^{-21}$	29 47	$2.8\cdot10^{-17}$ $1.2\cdot10^{-18}$	119 163	114 3.0	168 7.2
	1400	$1.0\cdot10^{-8}$ $1.1\cdot10^{-10}$	22 47	$1.0\cdot10^{-19}$ $2.3\cdot10^{-21}$	29 50	$1.4\cdot10^{-17}$ $5.7\cdot10^{-19}$	119 168	60 1.4	84 3.4
	2500	$6.4\cdot10^{-9}$ $4.2\cdot10^{-11}$	16 42	$6.5\cdot10^{-20}$ $7.7\cdot10^{-22}$	20 47	$6.5\cdot10^{-18}$ $1.8\cdot10^{-19}$	105 164	39 0.5	39 1.1
	4300	$3.6\cdot10^{-9}$ $2.3\cdot10^{-11}$	14 32	$4.7\cdot10^{-20}$ $3.3\cdot10^{-22}$	16 43	$3.8\cdot10^{-18}$ $7.0\cdot10^{-20}$	92 164	28 0.2	23 0.4
3000	1000	$5.8\cdot10^{-8}$ $2.6\cdot10^{-9}$	129 159	$3.3\cdot10^{-18}$ $1.8\cdot10^{-19}$	163 215	$2.7\cdot10^{-15}$ $1.9\cdot10^{-16}$	607 765	$2\cdot10^3$ 108	$1.62\cdot10^4$ $1.14\cdot10^3$
	1400	$3.6\cdot10^{-8}$ $1.3\cdot10^{-9}$	117 163	$1.9\cdot10^{-18}$ $9.4\cdot10^{-20}$	166 214	$1.5\cdot10^{-15}$ $1.0\cdot10^{-16}$	617 764	$1.14\cdot10^3$ 56	$9\cdot10^3$ 600
	2500	$1.6\cdot10^{-8}$ $4.8\cdot10^{-10}$	145 196	$6.7\cdot10^{-19}$ $3.1\cdot10^{-20}$	159 207	$5.3\cdot10^{-16}$ $3.2\cdot10^{-17}$	619 763	402 19	$3.18\cdot10^3$ 192
	4300	$6.5\cdot10^{-9}$ $2.3\cdot10^{-10}$	91 112	$2.6\cdot10^{-19}$ $1.1\cdot10^{-20}$	153 194	$2.0\cdot10^{-16}$ $1.0\cdot10^{-17}$	614 755	132 6.6	$1.2\cdot10^3$ 66

Note. The numbers in the first row correspond to perfect focusing, and those in the second row to the absence of focusing; N_{ev} is the number of events in a target of mass 10^6 ton or 6×10^{14} primary protons; N_μ is the number of equilibrium muons that pass through an area of 10^4 m^2 for 6×10^{14} primary protons.

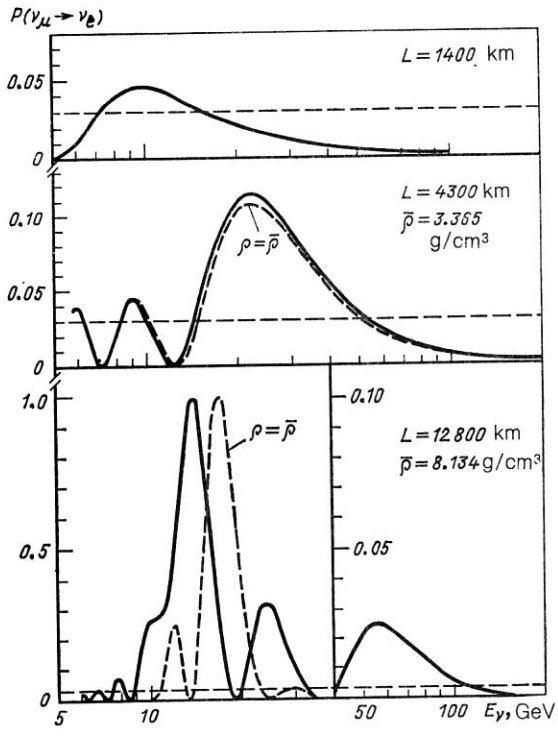

FIG. 28. Probability $P(\nu_\mu \to \nu_e)$ as a function of the neutrino energy for different distances for $\sin^2 2\theta = 0.03$, $\Delta m^2 = 0.01$ eV$^2/c^4$: the broken curves are calculated for a constant density $\bar{\rho}$ equal to the mean density on the corresponding chord; the broken lines are the amplitude of the vacuum fluctuations.

at a distance of about 7000 km the density varies relatively little and $\tilde{\rho}_c \simeq 10.5$ g/cm^3, $|\delta\rho|_{\max} \simeq 2.2$ g/cm^3. If $L_\nu/L_0(\bar{\rho}_c) = \cos 2\theta$, then the resonance is strongly manifested for $\Delta x \simeq 7000$ km $\gtrsim L_0/2 \tan 2\theta$ and $|\delta\rho|_{\max}/\bar{\rho}_c \lesssim \tan 2\theta$, i.e., for $\tan 2\theta \gtrsim 0.24$ and $\tan 2\theta \gtrsim 0.2$, respectively. Therefore, for $\sin^2 2\theta \gtrsim 0.05$ and $\Delta m^2/E_\nu \sim 0.8 \times 10^{-3}$ eV^2/(GeV$\cdot c^4$) the probability $P(\nu_\mu \to \nu_e)$ will be of order unity, as is confirmed by direct calculations. Bearing in mind that for the UNK the E_ν interval is $1 \leqslant E_\nu \lesssim 10^3$ GeV, we conclude that the interval of Δm^2 in which appreciable enhancement of the oscillations is possible is $10^{-3} \lesssim \Delta m^2 \lesssim 1$ eV$^2/c^4$.

For L equal to 1400 and 4300 km, the density is $\rho \simeq 2.5$–3.5 g/cm^2, and the corresponding length $L_0 \simeq 1.4 \times 10^4$ km is much greater than the chord length, so that the matter has a weaker influence on the oscillations.

The dependence of $P(\nu_\mu \to \nu_e)$ on the neutrino energy is shown in Fig. 28 for $\sin^2 2\theta = 0.03$ and $\delta m^2 = 0.01$ eV$^2/c^4$. For $E_\nu/\Delta m^2 \gg 10^4$ GeV$\cdot c^4$/eV^2 the matter suppresses the oscillations. If $E_\nu/\Delta m^2 \ll 10^3$ GeV$\cdot c^4$/eV^2 ($L_\nu/L_0 \ll 1$), the oscillations are close to the vacuum value. The broken curves correspond to a constant density equal to the mean density along the corresponding chord. It can be seen that for distances $L \lesssim 4300$ km the results for $\rho = \bar{\rho}$ is close to the exact solution of Eq. (9).

A clear picture of the oscillations in the matter of the earth is given by the dependence $P(\nu_\mu \to \nu_e)$, represented as a function of the two variables $\Delta m^2/E_\nu$ and $\sin^2 2\theta$. Figure 29 shows the contours $P(\nu_\mu \to \nu_e) = \text{const} = 10^{-1}$, 10^{-2}, and 10^{-3}. The matter "shifts" the contours relative to the vacuum case to larger values of $\Delta m^2/E_\nu$ for $\sin^2 2\theta \simeq 1$ and smaller $\sin^2 2\theta$ for $\sin^2 2\theta \ll 1$. This effect is particularly large when the neutrinos travel along the earth's diameter (Fig. 29c). This reduces the sensitivity of the experiment in the region $\sin^2 2\theta \approx 1$ but increases it at small mixing angles. By a simple change of scale of the ordinate one can obtain the contours $P(\nu_\mu \to \nu_e) = \text{const}$ for any fixed energy E_ν.

The isometric images of the surface $P_{\nu_\mu \to \nu_e}(\Delta m^2/E_\nu, \sin^2 2\theta)$ clearly demonstrate the influence of the earth's matter on the oscillations (Fig. 30).

In the real case of a neutrino beam with a broad spectrum it is necessary to average $P_{\nu_\mu \to \nu_e}(\Delta m^2/E_\nu, \sin^2 2\theta)$ over the spectrum. Since the dimensions of the neutrino source (the decay tunnel of the accelerator) are appreciably smaller than the oscillation length, the averaging over the region of formation of the neutrinos can be ignored.

Figures 31 and 32 show the results of calculations of the contours R_e, $R_\mu = \text{const} = 10^{-1}$, 10^{-2}, 10^{-3}, where R_e and R_μ are, respectively, the ratios, averaged over the neutrino spectrum, of the number of electrons produced in the volume of the detector (through the processes $\nu_\mu \to \nu_e$, $\nu_e N \to e + \ldots$) to the number of muons expected in the absence of oscillations, and the relative decrease in the flux of equilibrium muons due to the oscillations ($\nu_\mu \to \nu_X$, $\nu_\mu N \to \mu + \ldots$). It can be seen that the broad-band neutrino beams of the UNK can be used to look for oscillations in experiments with large L. For example, if after subtraction of the background the admixture of ν_e events among the ν_μ events is 0.1%, then at distance 4300 km for $E_p = 600$ GeV and ideal focusing the region of investigated parameters is, in accordance with Fig. 31g; $\Delta m^2 = 10^{-4}$ eV$^2/c^4$ ($\sin^2 2\theta = 1$) and $\sin^2 2\theta = 6 \times 10^{-4}$ ($\Delta m^2 = 10^{-2}$ eV$^2/c^4$).

Comparison of Figs. 31 and 32 shows that for otherwise identical conditions (E_p, L, type of focusing) the method of detection of ν_e events in the volume of the detector has a sensitivity to the parameter Δm^2 that is 2–3 times greater than for detection of the decrease in the flux of equilibrium muons. However, from the technical point of view the problem of detecting electrons in a detector of a large volume is incomparably more complicated than the problem of detecting equilibrium muons.

Enhancement of the oscillations by matter improves the sensitivity of the measurements. For example, for $L = 4300$ km the minimally attainable values of $\sin^2 2\theta$ are 1.5–2 times lower than the vacuum values for the same accuracy of the measurements. A particularly convenient method for the study of oscillations is the use of quasimonoenergetic neutrino beams.[109]

The time needed to accumulate the required statistics can be estimated by means of Table IV. For example, for $E_p = 600$ GeV, ideal focusing, and detector area $S = 10^4$ m^2 it is possible to detect about 5×10^5 muons at distance $L = 4300$ km during a month. This would permit measurement of a decrease of the muon flux at the level $\sim 1.5 \times 10^{-3}$ (statistical accuracy), and one could obtain the restrictions on Δm^2 and $\sin^2 2\theta$ in accordance with Fig. 31g.

Of course, it must be borne in mind that such accuracies can be ensured in a real experiment if there is effective monitoring of the neutrino beam, for which, in the case of a broad-spectrum beam, it is evidently necessary to have an additional "short-distance" neutrino detector near the accelerator. For a quasimonoenergetic beam a single detec-

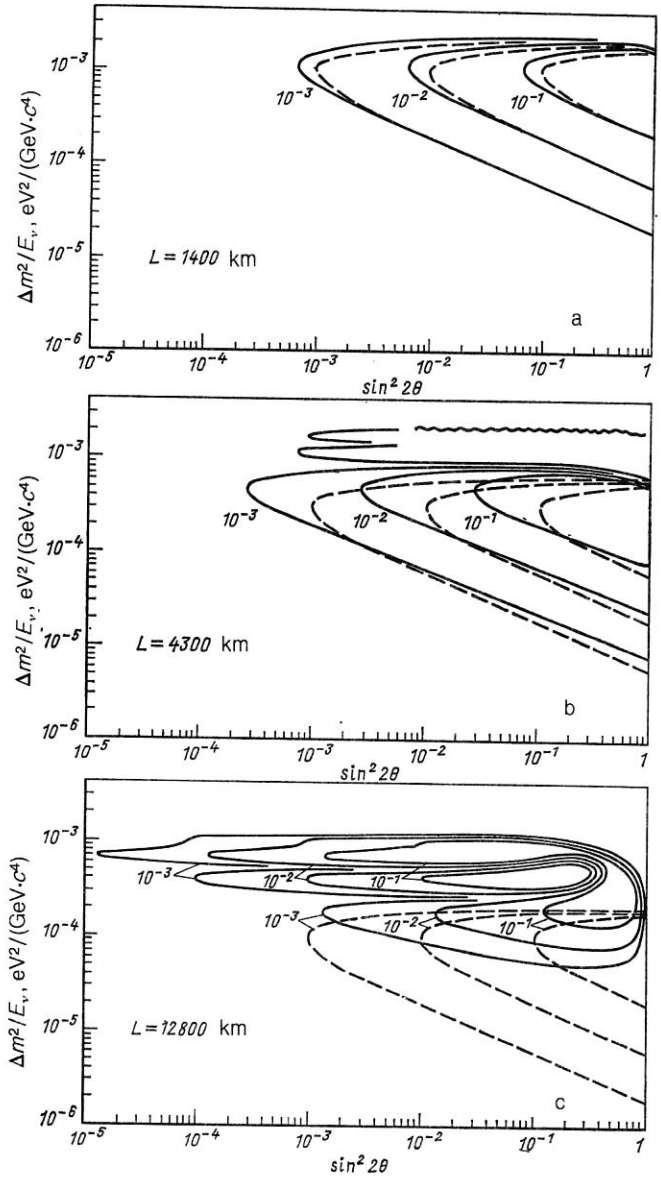

FIG. 29. Contours $P(\nu_\mu \to \nu_e) = \text{const} = 10^{-1}, 10^{-2}, 10^{-3}$ (the broken contours are for the vacuum).

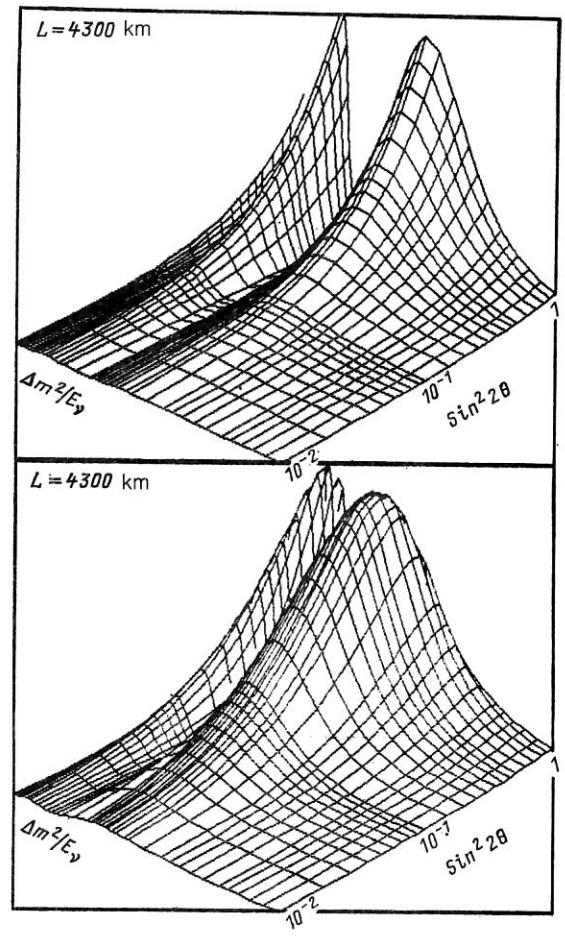

FIG. 30. The surface $P(\nu_\mu \to \nu_e)$ in the plane $(\Delta m^2/E_\nu, \sin^2 2\theta)$ (the upper figure gives the surface for the vacuum).

tor is in principle sufficient, since the variation of the energy can replace measurements at different distances.[108]

As regards the main "long-distance" detector, the most adequate would evidently be an underwater Cherenkov detector, which can ensure a large muon detection area, in particular a detector with light focusing,[115] though other detector types can also be used.

We have given above the results of a detailed quantitative analysis for oscillations in a system of two neutrinos. We now make some qualitative remarks for the three-neutrino case.

It is obvious that for $\Delta m^2_{21} > 0$ and $\Delta m^2_{31} > 0$ two resonances can arise in $\nu_e \to \nu_X$ transitions, and one in $\nu_\mu \to \nu_X$ transitions. They will be clearly expressed if they are "sufficiently separated,"[110] i.e., $\Delta m^2_{31} - \Delta m^2_{21} \gg \Delta m^2_{31} \sin\theta_{31} + \Delta m^2_{21} \sin\theta_{21}$ and $\sin^2\theta_{12} \ll 1$, $\sin^2\theta_{13} \ll 1$. For $\sin^2\theta_{23} \ll 1$ resonance at the lower density occurs in the $\nu_e \to \nu_\mu$ transition, whereas at the other density it occurs in the $\nu_e \to \nu_\tau$ transition. Under these conditions the $\nu_e \to \nu_\mu$ and $\nu_e \to \nu_\tau$ transitions are actually described by the two-neutrino probabilities calculated above (which must also be multiplied by a factor $\cos^2\theta_{23}$ to take into account the participation of a third neutrino). Since $P(\nu_e \to \nu_X) = 1 - P(\nu_e \to \nu_\mu) - P(\nu_e \to \nu_\tau)$, it follows that $P(\nu_e \to \nu_X)$ is sensitive to the matter effects for each of the ν_e transitions, whereas $P(\nu_\mu \to \nu_X)$ can be enhanced only by a single transition $(\nu_\mu \to \nu_e)$.

In the case of the reverse mass hierarchy,[96] one can expect enhancement of the oscillations for $\bar\nu_e \to \bar\nu_\mu, \bar\nu_\tau$. As was shown above, the condition for resonance in the earth is $(\Delta m^2/E_\nu)_{\text{res}} \simeq 0.8 \times 10^{-3}$ eV² (GeV·c⁴). Therefore, for energies $E \sim 10^1$–10^3 GeV the resonance mass interval of the heaviest neutrino (ν_3 or ν_1 in the direct or reverse hierarchies, respectively) is ~ 0.1–1 eV/c².

Violation of T invariance

As we have already noted, the masses and mixing angles in the lepton sector are directly related to the parameters of the neutrino oscillations. In the case of three generations, one of the mixing parameters is responsible for the violation of T invariance, and the corresponding effects can in principle be discovered in experiments with long-distance neutrinos, for which, in addition, they may be enhanced by the presence of matter.[110,111] It should be emphasized that in the

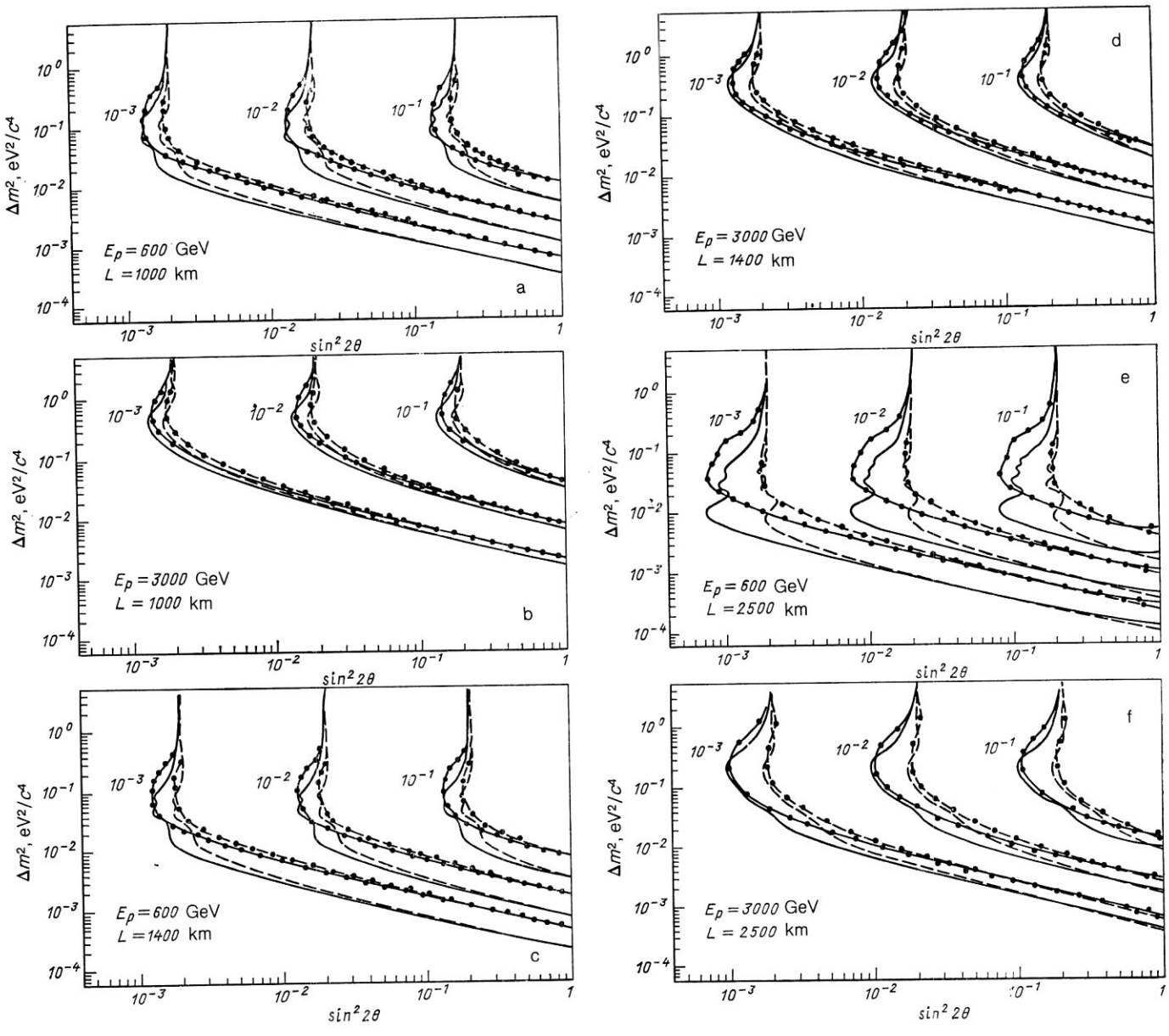

FIG. 31. Contours of $R_e(\Delta m^2, \sin^2 2\theta)$ for 10^{-1}, 10^{-2}, 10^{-3} for the relative number of ν_e events in the volume of the detector. The continuous curves represent calculations with allowance for the influence of the matter of the earth, and the broken curves represent the vacuum oscillations. The curves identified by the black dots are obtained for neutrino spectra without focusing of the mesons, while the curves without dots are for ideal focusing.

majority of astrophysical neutrino experiments one can observe only the transition probability for the electron neutrino, $\nu_e \to \nu_e$, which does not depend on the T-violating phase. Another feature that distinguishes experiments with long-distance neutrinos on the earth is the symmetry under the substitution $x \to -x$ for the matter in the path of the neutrinos; this is important for observation of the effect.

For example, suppose that the lepton mixing matrix U is parametrized in the form[110]

$$U = O^{23}(\varphi_{23})\, O^{33}(\delta)\, O^{13}(\varphi_{13})\, O^{12}(\varphi_{12});$$

$$O^{33}(\delta) = \begin{pmatrix} 1 & 0 & 0 \\ 0 & 1 & 0 \\ 0 & 0 & e^{i\delta} \end{pmatrix}; \quad O^{12}(\varphi_{12}) = \begin{pmatrix} \cos\varphi_{12} & \sin\varphi_{12} & 0 \\ -\sin\varphi_{12} & \cos\varphi_{12} & 0 \\ 0 & 0 & 1 \end{pmatrix};$$

$$O^{13}(\varphi_{13}) = \begin{pmatrix} \cos\varphi_{13} & 0 & \sin\varphi_{13} \\ 0 & 1 & 0 \\ -\sin\varphi_{13} & 0 & \cos\varphi_{13} \end{pmatrix};$$

$$O^{23}(\varphi_{23}) = \begin{pmatrix} 1 & 0 & 0 \\ 0 & \cos\varphi_{23} & \sin\varphi_{23} \\ 0 & -\sin\varphi_{23} & \cos\varphi_{23} \end{pmatrix}.$$

The presence of a phase δ not qual to 0 or π leads to violations of CP and T invariance, and these are manifested in oscillations:[92,93,116]

$$P(\nu_l \to \nu_{l'}) \neq P(\bar{\nu}_l \to \bar{\nu}_{l'}) \tag{10a}$$

and

$$P\overset{(-)}{(\nu_l} \to \overset{(-)}{\nu_{l'}}) \neq P\overset{(-)}{(\nu_{l'}} \to \overset{(-)}{\nu_l}); \tag{10b}$$
$$l \neq l' = e,\ \mu,\ \tau.$$

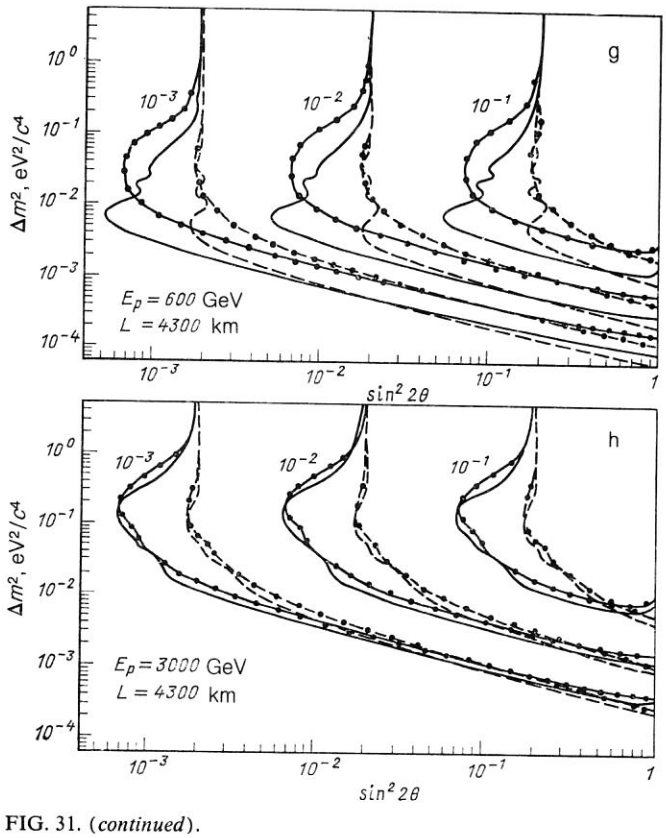

FIG. 31. (*continued*).

In matter the relation (10a) can arise even when $\delta = 0$, since the matter of the earth is not C-symmetric, and the interaction of neutrinos with it is not invariant with respect to the CP and CPT transformations.[117] This means that the existence of the CP-and T-violating phase δ can be indicated only by observation of the asymmetry in the oscillations that is due to T violation:[110,111]

$$\overset{(-)}{A}{}^{(l'l)}_{T} = P\,(\overset{(-)}{\nu}_l \to \overset{(-)}{\nu}_{l'}) - P\,(\overset{(-)}{\nu}_{l'} \to \overset{(-)}{\nu}_l).$$

It follows from unitarity that in the oscillations in a system of three neutrinos (or antineutrinos) we have[110]

$$\overset{(-)}{A}{}^{(\mu e)}_{T} = \overset{(-)}{A}{}^{(\tau\mu)}_{T} = \overset{(-)}{A}{}^{(e\tau)}_{T} \equiv \overset{(-)}{A}_{T}. \tag{11}$$

In vacuum

$$A^V_T = -\bar{A}^V_T = 4J^V\left[\sin\frac{\Delta m^2_{21}}{2E}\,R + (31) + (23)\right];$$

$$J^V = \frac{1}{8}\sin\delta\sin 2\varphi_{12}\sin 2\varphi_{13}\sin 2\varphi_{23}\cos\varphi_{13}.$$

As with the situation in the quark sector, we find that C and TP invariance holds ($A^{(-)V}_T = 0$) if: a) $\delta = 0,\ \pi$; b) $m_{\nu_i} = m_{\nu_j}$; c) $\varphi_{ij} = 0$ or $\pi/2$.

The presence of matter modifies the relations derived above.[110,111] In particular, in the simplest case with matter of constant density the form of (11) remains unchanged, but the parameters δ and φ_{ij} in (11) must be replaced by the corresponding values in the matter. At the same time, A^m_T is nonvanishing only if $A^V_T \neq 0$. If the mixing angles φ^m_{ij} are increased, the matter can increase the asymmetry, $|A^m_T| > |A^v_T|$, for example, if $\sin\varphi_{12,13} \ll 1$ but $\sin 2\varphi^m_{12}$ and $\sin 2\varphi^m_{13}$ are both enhanced in the matter (for this Δm^2_{21} and Δm^2_{31} must not differ strongly).

These effects are illustrated by Fig. 33 (from Ref. 110). The ratio I_T, which characterizes the asymmetry, is defined as

$$I_T = \frac{P(\nu_e \to \nu_\mu) - P(\nu_\mu \to \nu_e)}{P(\nu_e \to \nu_\mu) + P(\nu_\mu \to \nu_e)}.$$

We see that there exists a fairly broad range of values of the parameters which characterize the oscillations in the three-neutrino system in which the effects of the T violation can be considerably enhanced if the neutrino beams pass through the earth and are detected in experiments with long-distance neutrinos.

Decay of neutrinos in matter

Experiments with long-distance neutrinos can be used to look for neutrino decays due to interaction with matter.[118] If N_e and N_n are the electron and neutron densities of the matter, then the motion of neutrinos in this matter can be described by a Dirac equation analogous to the equation for an electron in an external field: $eA_\mu = (\rho, 0)$ where for ν_e we have $\rho = G\sqrt{2}N_e - \rho',\ \rho' = -GN_n/\sqrt{2}$, and for ν_μ and ν_τ we have $\rho = \rho'$. Since the ν and $\bar{\nu}$ scattering amplitudes have opposite signs, the ν and $\bar{\nu}$ energy levels in matter are also different:

$$E_{\nu/\bar{\nu}} = \sqrt{p^2_\nu + m^2_\nu c^4} \pm \rho. \tag{12}$$

As a result, in matter decays of ν (or $\bar{\nu}$, depending on the neutrino species and N_n) are energetically possible and are accompanied by emission of a massless (or fairly light) scalar particle, for example, a Majoron:[119] $\nu \to \bar{\nu} + \alpha$ or $\bar{\nu} \to \nu + \alpha$. (The diagonality of the Majoron couplings preclude such decays in vacuum.)

Beams of accelerator neutrinos consist mainly of muon neutrinos. It can be seen from (12) that in matter $\bar{\nu}_\mu$ is heavier than ν_μ, and the decay $\bar{\nu}_\mu \to \nu_\mu + \alpha$ is possible, i.e., for an experiment one needs a $\bar{\nu}_\mu$ beam. A restriction on the $\bar{\nu}_\mu \to \nu_\mu + \alpha$ decay probability can be obtained from data on the $K \to \mu\nu$ decay, from which it follows that $\tau_{\bar{\nu}_\mu \to \nu_\mu \alpha} \simeq 50$ sec. Therefore, as neutrinos traverse the earth's diameter, decay of about 1% of the $\bar{\nu}_\mu$ can be expected. It is rather difficult to detect such a decrease in the $\bar{\nu}_\mu$ flux, but for the identification of the transformations $\bar{\nu}_\mu \to \nu_\mu$ that occur a very clear signature is available, namely, production of muons of the opposite sign (i.e., μ^-), $\nu_\mu n \to \mu^- + X$, instead of the μ^+ mesons expected from $\bar{\nu}_\mu$. Therefore, the detector must distinguish μ^+ and μ^-. The existence of the effect does not depend on the neutrino mass and, in particular, will also occur for massless neutrinos. The probability of decay in matter does not depend on the neutrino energy (whereas for ordinary decays in vacuum $\Gamma \sim E_\nu^{-1}$), and the energy E_ν can be chosen on the basis of considerations relating to the production of the beam and its detection at large distances.

Heavy neutrinos

The possibility of looking for and measuring the mass of a heavy neutrino using the time of flight in beams of long-distance neutrinos was discussed in Ref. 120. If the neutrino has energy E_ν, then over a base of length L the difference between the times of flight for a massless neutrino and a neutrino with mass M is $\Delta t \simeq (L/2c)(Mc^2/E_\nu)^2$. If the time of flight can be measured to an accuracy of, say, ~ 1 nsec (the operation of the accelerator and detector must be synchronized to such an accuracy), then for detection of a neu-

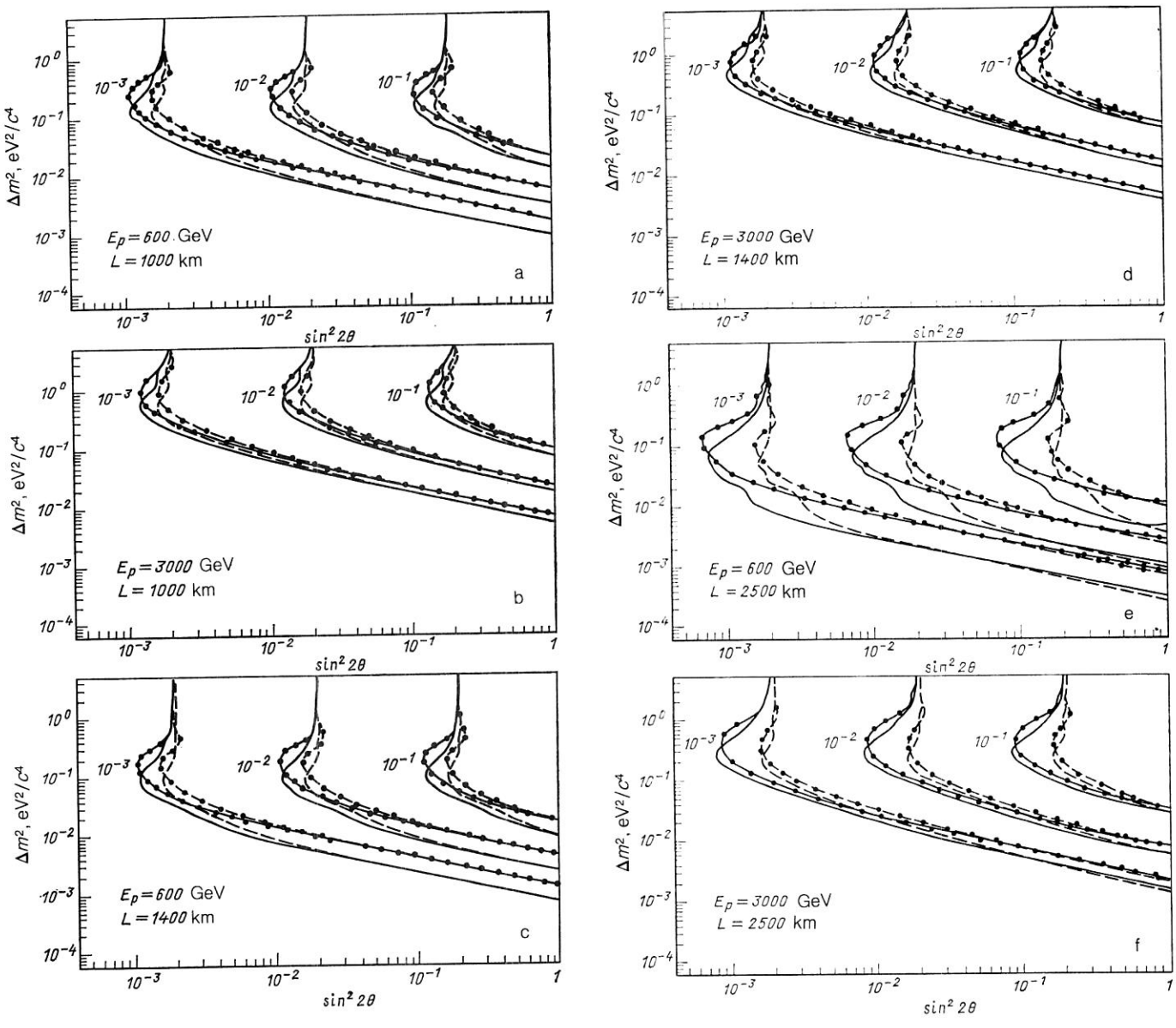

FIG. 32. Contours of $R_\mu(\Delta m^2, \sin^2 2\theta)$ for 10^{-1}, 10^{-2}, 10^{-3} for the relative decrease in the flux of equilibrium muons. For the notation, see the previous figure.

trino with $E_0 = 2$ GeV and $L = 10^4$ km a restriction $M \lesssim 1$ MeV/c^2 on the neutrino mass can be obtained. In principle, such accuracy can be achieved for the UNK. The signals from the delayed (heavy) neutrinos arrive in the gaps between the pulses due to the accelerator bunches.

4. NEUTRINO GEOPHYSICS

Besides the investigations into neutrino physics, beams of long-distance neutrinos from the UNK open up the first real possibility for making fundamental and applied investigations in "neutrino geophysics."[102-107]

The inclusion of such investigations in the neutrino program of the UNK would be of undoubted interest. Geophysical applications are discussed in detail in the reviews of Refs. 102 and 105–107, and for completeness we shall here mention briefly some of them, going into slightly more detail for only the question, which is related to the neutrino oscillations in the matter of the earth discussed above.

Geodesy

Beams of long-distance neutrinos give in principle a possibility to make high-precision geodesic measurements on the scale of the earth.[121] The method is based on measurement of the time of flight of neutrinos from the source to the detector. The necessary condition—the synchronization of the operation of the accelerator and the detector to a high accuracy—can be achieved by means of time standard or satellites. Such measurements are of undoubted interest for the solution of numerous geophysical problems: study of the diurnal tidal vibrations of the earth, which have an amplitude of about 50 cm; motions of tectonic plates, in particular of faults, and the correlations of this motion with seismic activity; the relative motion of points on different continents, vertical displacement of the ocean floor, etc.

The beams from the UNK could be used both to solve real geophysical problems and to develop methods of mea-

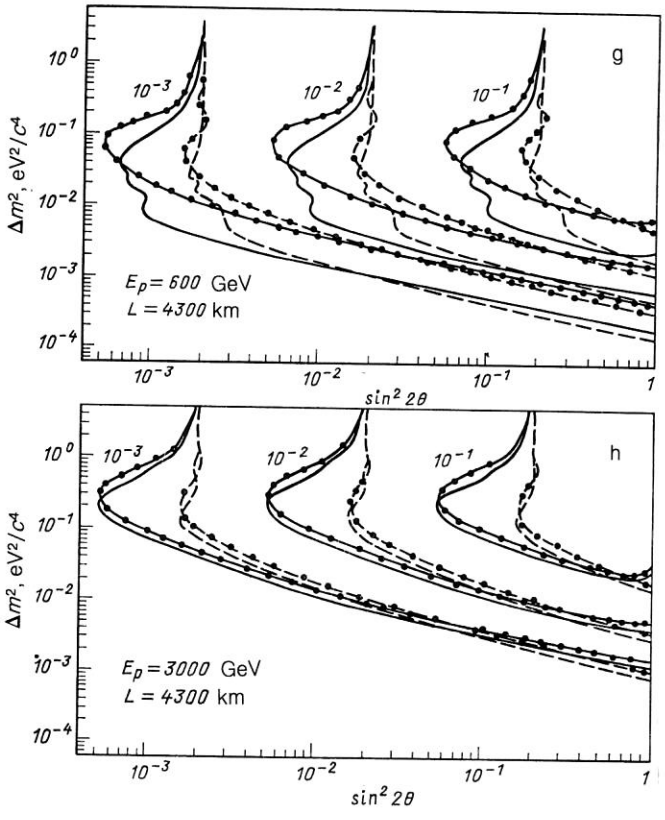

FIG. 32. (*continued*).

surements (synchronization, recovery of trajectories with allowance for distortions on detection, etc.).

Investigation of the structure of the earth

The penetrating power of neutrinos makes possible global investigation of the earth's structure by means of beams of long-distance neutrinos. The most direct method is the one in which one determines from the absorption the total mass of matter (per unit area) along different chords of the terrestrial ball and from these data recovers the matter density distribution $\rho(x)$.[103,104] The method is effective at sufficiently high energies, since the relative change in the neutrino flux due to absorption even along the terrestrial diameter is small: $\Delta J/J \simeq 0.06\,(E/\text{TeV})$. Nevertheless, such measurements can be made in the UNK beams if sufficiently large detectors are used (for example, underwater Cherenkov detectors); in fact, one can achieve $\Delta M/M \simeq 3\%$ for $s_d \sim 10^4$ m^2 during a run of 1–3 months. (More detailed discussions of such measurements can be found in Refs. 102, 105, and 106.)

Another proposed method is based on measurement of the oscillation effects in matter and their strong dependence on the matter density along the neutrino beam.[109,112]

As can be seen from Fig. 34, for $\Delta m^2/E_\nu \simeq 0.77\times 10^{-3}$ eV^2(GeV·c^4) the value of P is very sensitive to changes in ρ: $P(M) \simeq 0.6$, $P(1.1M) \simeq P(0.9M) \simeq 0.4$. Accordingly, the relative change in the number of neutrinos and muons accompanying them will in this case be $\Delta N_\mu/\bar{N}_\mu \simeq 0.4$. It is important that this value exceeds the relative uncertainty in the neutrino flux. Requiring that ΔN_μ exceed the statistical uncertainty, $\delta N_\mu \simeq \sqrt{N_\mu}$, we can estimate the time needed to measure M to accuracy $\delta = \delta M/M$:

$$t(\delta) = \left\{ \frac{d\bar{N}_\mu}{ds\,dt}\, s_d \left(\frac{\Delta N_\mu}{\bar{N}_\mu} \right)_\delta^2 \right\}^{-1},$$

where $d\bar{N}_\mu/dsdt$ is the flux density of the equilibrium muons, and s_d is the area of the detector. Naturally, to measure M in "oscillation" experiments the width of the neutrino spectrum must be less than the width of the resonance peak in Figs. 28 or 34: $\Delta E_\nu/E_\nu \lesssim 0.2$. The width of the quasimonoenergetic neutrino beam at the UNK can satisfy these requirements perfectly well. As regards the broad-band neutrino beam, for it a change in M leads merely to a displacement of the region of neutrino energies in which there is a significant decrease in the ν_μ flux, while the total number of ν_μ and, accordingly, of muons changes little.

Near resonance, the expected effects are of order unity. At the same time, at energies of hundreds of giga-electronvolts the absorption of the neutrinos is only fractions of a percent. Therefore, in the region of UNK energies the oscil-

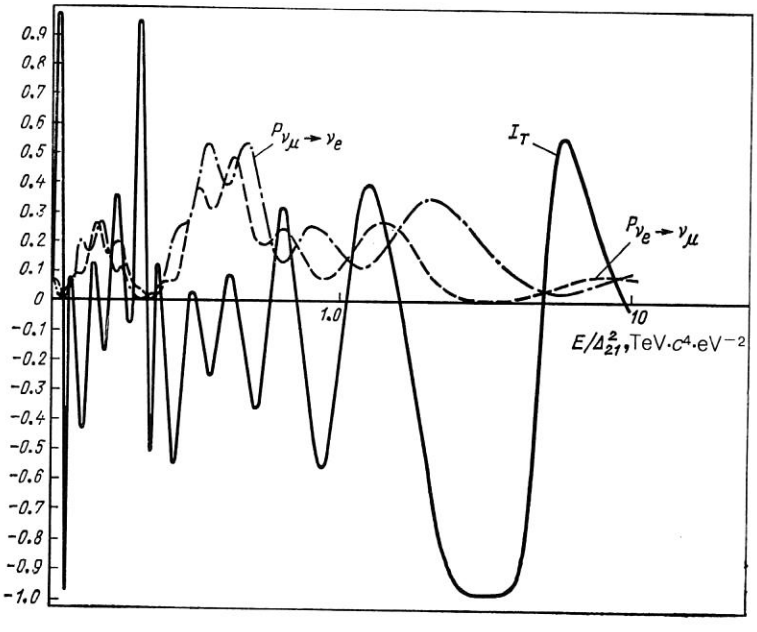

FIG. 33. Asymmetry I_T due to violation of T parity and the probabilities $P_{\nu_e \to \nu_\mu}$ and $P_{\nu_\mu \to \nu_e}$ as functions of $E/\Delta m^2_{21}$ for $\sin\varphi_{12} = 0.25$, $\sin\varphi_{13} = 0.2$, $\sin\varphi_{23} = 0.3$, $\delta = \pi/3$, and $\Delta m^2_{31} = 3\Delta m^2_{21}$ (Ref. 110).

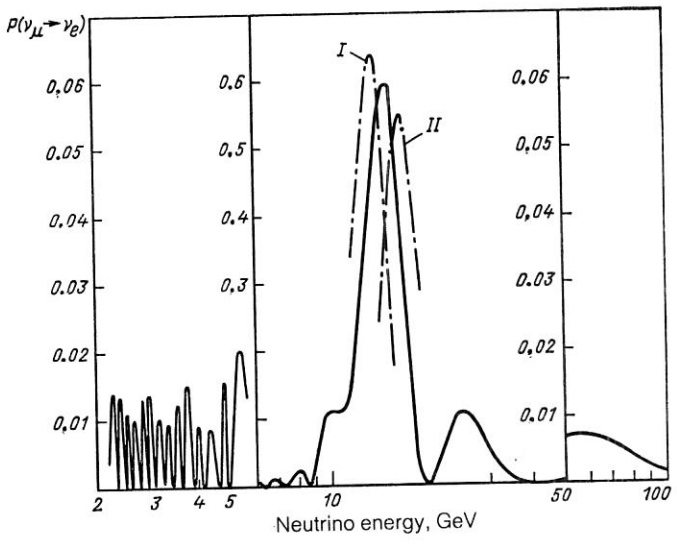

FIG. 34. Probability $P(\nu_\mu \to \nu_e)$ as a function of the energy for $\Delta m^2 = 10^{-2}$ eV$^2/c^4$, $x_0 = 12\,800$ km, $\sin^2 2\theta = 10^{-2}$. For the left and right sides of the figure the scale has been increased by ten times; the chain curves I and II are for the density distributions $\rho'(x) = 1.2\rho(x)$ and $\rho''(x) = 0.9\rho(x)$, respectively.

lation method of measuring M could be at least 1000 times more sensitive and "rapid" than the absorption method.[109]

Another remarkable feature of the oscillation method is the possibility of determining the linear distribution of the matter density along the neutrino beam.[112] In the absorption method only the total mass M of the matter along the path of the beam is measured. Therefore, to find the profile of the earth's density distribution $\rho(r)$ it is necessary to make measurement along different chords, and technically this is very difficult, since it requires displacement of the detector and realignment of the beam.

In contrast, in the oscillation method it is sufficient for the determination of $\rho(r)$ (under the assumption of spherical symmetry) to measure $P(x)$ along the earth's diameter, varying only the energy. From the point of view of the Schrödinger equation (9), this problem is the analog of the inverse scattering problem in quantum mechanics for fixed orbital angular momentum.[112] However, the direct use of the standard methods of the inverse problem is impossible for (9), since the effective potential $V(k,x)$ is complex and depends on x.

We consider the case that is most interesting from the practical point of view: $\sin 2\theta \ll 1$. In the limit $\cos 2\theta \to 1$, Eq. (9) has an obvious solution that satisfies the initial conditions (9'):

$$\psi_k(x) \simeq k \sin 2\theta \int_0^x \exp\{i[\bar{\varphi}(x') - \tilde{\varphi}(x)/2]\}\, dx';$$

$$\tilde{\varphi}(x) = 2\int_0^x dx' \left(\frac{1}{l(x')} - k\right). \qquad (13)$$

For the case considered here, in which the beam passes through the earth, it can be assumed that the density distribution is symmetric relative to the center: $\rho(x) = \rho(D - x)$. Then for the point of observation $x = D$ we have

$$\left.\begin{aligned} &\psi_k(D) = q \sin 2\theta f(q); \quad f(q) = \int_0^1 \cos[\varphi(\xi) - q\xi]\, d\xi; \\ &q = kD; \quad \varphi(\xi) = \frac{GN_A D}{2\sqrt{2}} \int_0^\xi \rho(\xi')\, d\xi'. \end{aligned}\right\}$$

In this case, $\psi_k(D)$ is real (a fact that does not depend on the approximation $\sin^2 2\theta \ll 1$), so that if the probability $P_k(D)$ is known, we have $\psi_k(D) = \pm\sqrt{P_k(D)}$. The sign of the square root changes each time the function $P_k(D)$ passes through zero. The reciprocal problem reduces to solution of the integral equation (14) and differentiation of the resulting function $\varphi(\xi)$.

Equation (14) has the form of a Fourier transformation defined only for $q > 0$ ($0 < E < \infty$). If the density were constant, then $\varphi(\xi) = \varphi(1)\xi$, and

$$f_0(q) = \frac{\sin(q - \varphi(1))}{q - \varphi(1)}.$$

For the case $\varphi(1) \gg 1$ it is sensible to extend the definition of $f(q)$ to $q < 0$: $f(q < 0) = f_0(q)$. Then for $q < 0$ the difference $f(q) - f_0(q)$ vanishes, and the inverse Fourier transformation gives

$$\int_0^\infty dq \left[f(q) - \frac{\sin(q - \varphi(1))}{q - \varphi(1)}\right] \sin q\xi$$

$$= \pi\{\sin\varphi(\xi) - \sin[\varphi(1)\xi]\}. \qquad (15)$$

In Ref. 112, this method was tested numerically. The distribution of the density ρ along the earth's diameter shown in Fig. 35 was taken as $\rho(x)$. For $\int_0^D \rho(x)dx = 1.04 \cdot 10^{10}$ g/cm^2, $\varphi(1) = 9.35$ and this justifies the definition of $f(q < 0)$ used above. For $\Delta m^2 = 10^{-2}$ eV$^2/c^4$ and $\sin^2 2\theta = 10^{-2}$, Eq. (9) was solved (numerically) or the solution (13) was used; the results were similar (Fig. 36). The resulting $f(q)$ was substituted in (14), from which the function $\varphi(\xi)$ was found, and then $\rho(r)$ was determined by differentiation. It can be seen from Fig. 35 that the approximate solution determines the main features of the distribution.

We have assumed above that Δm^2 is known exactly. To perform these experiments to measure $\rho(r)$, the relative error with which Δm^2 is known must be much less than the relative width of the resonance peak for $\Delta m^2/E_\nu \sim 10^{-3}$

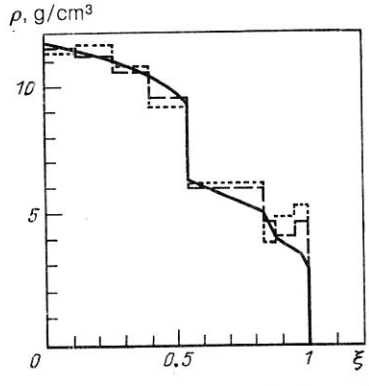

FIG. 35. Density distribution along the earth's diameter [$\xi = 2(x - D/2)/D$], $D = 12\,800$ km. The continuous line is the original density distribution; the broken line is the recovered density, $0 < q < 100$; the dotted line is for $0 < q < 20$.

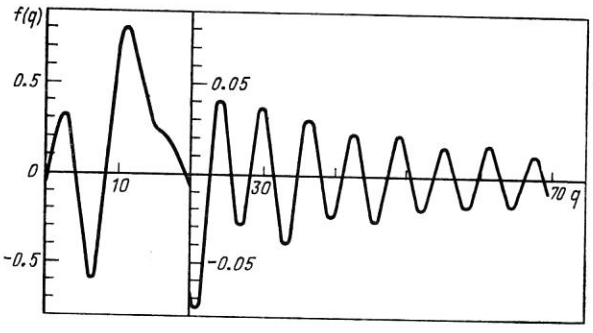

FIG. 36. The function $f(q)$ (14) for $\Delta m^2 = 10^{-2}$ eV$^2/c^4$, $\sin^2 2\theta = 10^{-2}$.

eV^2/(GeV·c^4), i.e., $\delta\Delta m^2/\Delta m^2 \ll 0.2$. The requirements on the accuracy in the determination of $\cos 2\theta$ are about the same: $\delta \cos 2\theta / \cos 2\theta \ll 0.2$.

In exactly the same way, measurement of the oscillation parameters Δm^2 and $\sin^2 2\theta$, in its turn, requires sufficiently good knowledge of ρ. The estimates of Ref. 109 show that for $\delta M/M \lesssim 0.2$ it is possible to measure Δm^2 to an accuracy of order 10%. For the simultaneous determination of Δm^2, $\sin^2 2\theta$, and ρ it is necessary to combine experiments with different $\Delta m^2/E_\nu$ and ρ, including experiments in the surface layers of the earth, where ρ is well known.

The principal difference between neutrino probing of the earth and traditional seismic probing is the possibility of a model-independent determination of $\rho(r)$.[102,107] At the same time, combination of the data of neutrino and seismic investigation will also permit determination of the compression and shear moduli and, therefore, will give information about the state of the matter in the depths of the earth. Finally, combined use of ν_μ and $\bar{\nu}_\mu$ beams will make it possible to estimate the mean number of protons and neutrons in different regions within the earth,[104,102] a possibility that is important for the determination of their element composition.

Secondary studies using beams of long-distance neutrinos

a) *Muons.* The muon flux generated by the neutrinos in the upper layers of the earth's crust can be used to look for deposits of heavy ores at depths from hundreds of meters to a few kilometers.[102,105] The conditions of such a search depend on the beam energy and on the distance of the investigated region from the accelerator, which may be hundreds or thousands of kilometers. The presence of a deposit could be signaled by a disturbance of the equilibrium muon flux due to a combination of two effects: an excess of neutrons and an increase in the stopping losses in matter with high atomic number. The method can be improved by measuring the spectral composition of the muons; this increases the sensitivity of the method and gives information about the depths of the deposit (deduced from the maximal energy of the muons) and the thickness of the stratum (deduced from the smearing of the upper limit of the spectrum).[122]

The UNK beams will make it possible to carry out investigations to small depths (hundreds of meters for $L \sim 10^3$ km), which would evidently be of a methodological nature.

b) *Acoustic signal.* The interaction of neutrinos with matter leads to the release of energy in the region through which the neutrino beam passes and to the formation of a (very weak) acoustic wave.[102,105,123] The wave amplitude from one pulse of the UNK accelerator at distance $h \simeq 1$ km from the beam and for $L \sim 10^3$ km is about 10^{-10} Pa (in a frequency range $\sim$1–100 Hz). The ratio of the signal to the seismic noise is very low, at the level 10^{-4}–10^{-6}. Nevertheless, there is a hope that the use of special methods to identify signals and accumulate them will open up a real prospect of detecting acoustic signals from beams of long-distance neutrinos of future accelerators. The geophysical use (for example, for prospecting for oil and gas deposits) is based on the fact that the acoustic signal carries information about the properties of the rocks in which it was generated and of the rocks through which it passes.[105]

Beams from the UNK will make it possible to carry out methodological studies at distances of about 10–50 km from the accelerator and at depth $h \lesssim 100$ m, where the acoustic signal will be $\sim 10^{-4}$ Pa, a value that corresponds approximately to the level of the seismic noise.

Distinctive effects could occur when neutrino beams interact with a seismically active region, for which neutrino interactions could play the part of a "trigger mechanism," leading to release of the elastic energy stored in such a region.[107,124] In this case the acoustic response could exceed the thermoacoustic signal by many orders of magnitude. There is a prospect that this could be used both for prospecting and to investigate seismic activity. If, as is assumed, a seismically active region also extends into the aseismic regions, this mechanism could be investigated with the UNK beams.

c) *Electromagnetic radiation in the ground and in the atmosphere.* In a number of problems with "long-distance" neutrinos it may be helpful, for detection of the neutrino beam, to use electromagnetic radiation (in the optical or radio ranges) generated by cascades from neutrino interactions.[102,107,125]

The power of the radio radiation in the ground from a single UNK pulse is very low, or order 10^{-14} W in the wavelength range $\lambda \sim \Delta\lambda \sim 10$ km; the emission angle is ~ 1 rad. In the centimeter range the radiation power increases by 4–6 orders of magnitude, but such waves are strongly absorbed in the ground.

The radio emission of neutrino beams in the atmosphere has a power that is 3–4 orders of magnitude lower than in the ground, and is mainly directed forward.[126]

The Cherenkov emission in the optical range in the atmosphere[126,127] is fairly intense for the UNK beams and could be detected (under appropriate background conditions), for example, by means of photomultipliers equipped with a reflector with a diameter of order ~ 1 m. Investigations involving the detection of optical radiation from beams of long-distance neutrinos from the UNK could be made on satellites, balloons, aircraft, and on the surface of the earth. They could serve as preparatory work for projects of the SHALON type,[127] which have the aim of detecting natural neutrinos.

Completing this section devoted to possible investigations with long-distance neutrinos, we should like to remark that the program of work proposed at the present time may not be particularly extensive. However, it should be borne in mind that the discussion of the problems associated with long-distance neutrinos began comparatively recently and as yet lacks the stimulating effect of real experiments with such neutrinos. It is to be hoped that as the work in this direction

develops many new interesting fundamental problems and practical applications that at the present time we do not anticipate will come to light.

In the first stage, after the commissioning of the UNK, the most important problem could be the mastering of the technology of long-distance neutrinos—the construction of a neutrino channel and of the system for directing the beam, the time synchronization, the detectors, and the gaining of the first experience of operations with long-distance neutrinos. Later the program could combine studies in fundamental and applied directions, which, mutually enriching and sustaining each other, could simultaneously stimulate the development of supporting techniques and technology.

It cannot be doubted that sooner or later beams of long-distance neutrinos will be mastered. Work with long-distance neutrinos from the UNK could be the first step in this direction.

5. REMARKS ABOUT THE POSSIBILITY OF NEUTRINO INVESTIGATIONS AT THE UNK IN THE COLLIDER REGIME

In conclusion, we assess the possibility of carrying out neutrino experiments when the UNK accelerator is operated in the collider regime. Although colliders have an undoubted advantage, the high collision energy, their shortcoming is the absence of secondary beams, including lepton beams, and this greatly reduces the possibilities for experimental investigation. In Ref. 128 attention was recently drawn to the fact that in multi-TeV colliders this shortcoming can be at least partly compensated by using high-energy and well-collimated beams of direct leptons that are generated at the positions at which the $p\bar{p}$ beams collide. The role of direct neutrinos in the formation of the neutrino beams of high-energy accelerators was already noted in Ref. 129. The advantage of direct neutrinos over ordinary neutrinos from decays of π or K mesons at high energies is based on the appreciable difference between the decay lengths of ordinary hadrons and charmed particles. The typical decay length of the latter for mass $m_c \simeq 2$ GeV/c^2 and lifetime $\tau_c \simeq 5\times 10^{-13}$ sec at UNK energies is[5)]

$$l_c = \gamma c\tau_c \simeq 4.5\,[5/(n+2)]\,E_p,$$

i.e., for $n = 1$–5 we have $l_c \simeq 3$–10 cm. At the same time, the pion decay length (in km)

$$l_\pi = \gamma c\tau_\pi \simeq 28\,[6/(n_\pi + 2)]\,E_p$$

is equal to 28 km for $n_\pi = 4$. Therefore, for $\sigma_c/\sigma_{\text{tot}} \simeq 0.1$ and a length of the order of a hundred meters for the straight section of the $p\bar{p}$ collider the ratio of the number of leptons from pion decay and of charmed particles is $\sim 1/10$, and at shorter lengths the direct generation is completely predominant. The mean energy of the direct neutrinos can be estimated in accordance with the formula $\langle E_l\rangle = E_p/(3n+6)$. However, the most accurate Monte Carlo calculations[128] give a somewhat smaller (by $\sim 15\%$) value of $\langle E_\nu\rangle$, and this is taken into account in Table V.

The lepton flux can be found from the formula[128]

$$\Phi_e = \Phi_0 \frac{\sigma(C)}{\sigma_c} BR\,(C \to l),$$

where

$$\Phi_0 = \frac{1}{2} L\sigma_{\text{tot}} \frac{\sigma_c}{\sigma_{\text{tot}}};$$

L is the luminosity of the collider (for the UNK, we take $L = 10^{33}$ cm$^{-2}\cdot$sec^{-1}). For the remaining quantities, σ_{tot} is the total cross section of the $p\bar{p}$ interaction, σ_c is the total cross section for the production of the charmed particles, $\sigma(C)$ is the cross section for the production of the charmed particles of a definite species ($D,\bar{D},\Lambda_c,F^{\pm}$), and BR is the decay branching ratio (we use the values from Ref. 128). In particular, $\sigma_{\text{tot}} = 38.3 + 0.5\ln^2(S/116\ \text{GeV}^2)$, and for the UNK $\sigma_{\text{tot}} \simeq 118.24\times 10^{27}$ cm^2. Setting $\sigma_c/\sigma_{\text{tot}} = 0.1$, we obtain

$$\Phi_0 = 5.9\cdot 10^6\ \text{sec}^{-1}.$$

The number of neutrino interactions during the time T in a detector of length l with transverse dimensions greater than the beam width [the angular opening of the lepton beam is 2 mrad (3 TeV/E_p)] and with matter density ρ is

$$N = \rho N_A \cdot 10^{-35}\ \text{cm}^2\ \langle E_\nu\rangle\,\Phi_\nu lT$$

($N_A = 6\times 10^{23}$ nuclei/g is Avogadro's number). Taking $T = 10^7$ sec (one year), $l = 25$ m, and $\rho = 5$ g/cm^3, we obtain

$$N \simeq 0.375\ \langle E_\nu\rangle\,\Phi_\nu.$$

In Table VI we give the results of estimates for the UNK[130] of the number of events in the detector due to direct neutrinos from the various decays. For comparison we give the analogous results[128] for the colliders LHC (8 TeV×8 TeV) and SSC (20 TeV×20 TeV) at the same luminosity.

In the final column of Table VI we give estimates for the number of neutrino interactions in experiments of the beam-dump type that could be performed when the beam is "dumped." Then[128]

$$\Phi_l\,(bd)/\Phi_l = \frac{365d}{\pi 10^7 c} N_p \left(\frac{\sigma_c}{\sigma_{\text{tot}}}\right)_{bd} \frac{1}{\Phi_0},$$

where N_p is the total number of protons spilled onto the target, and d is the number of spills in a day. Taking for the UNK the number of protons in the ring to be $N_p = 2.5\times 10^{13}$, $d = 3$, and the ratio $(\sigma_c/\sigma_{\text{tot}})_{bd} \simeq 0.015$ for $E_p = 3$ TeV, we obtain

$$\Phi_l\,(bd)/\Phi_e \simeq 2.2\ (d/3)\ (N_p/2.5\cdot 10^{13}).$$

We also give an estimate of the main "background"—the

TABLE V. Mean energy, TeV, of direct neutrinos.

$D \to \nu_\mu, \nu_e$ $\bar{D} \to \bar{\nu}_\mu, \bar{\nu}_e$ $(n = 2)$	$\Lambda_c \to \nu_\mu, \nu_e$ $(n = 0,5)$	$F^+ \to \tau^+ \to \bar{\nu}_\tau$ $F^- \to \tau^- \to \nu_\tau$ $(n = 2)$	$F^+ \to \nu_\tau$ $F^- \to \bar{\nu}_\tau$ $(n = 2)$
0.23	0.37	0.24	0.07

TABLE VI. Number of interactions per year from direct neutrinos at the UNK, LHC, and SSC.

Accelerator	ν_e from D (ν_μ from D)	$\bar{\nu}_e$ from $\bar{D}$ ($\bar{\nu}_\mu$ from $\bar{D}$)	ν_e from F^+ (ν_μ from F^+)	$\bar{\nu}_e$ from F^- ($\bar{\nu}_\mu$ from F^-)	ν_e from Λ_c (ν_μ from Λ_c)	Total number of interactions	Number of interactions in beam-dump
UNK	$2.6\cdot10^4$	$1.4\cdot10^4$	$1.9\cdot10^4$	$1.0\cdot10^4$	$1.9\cdot10^4$	$1.8\cdot10^5$	$4\cdot10^5$
LHC	$8.4\cdot10^4$	$4.6\cdot10^4$	$6.3\cdot10^4$	$3.5\cdot10^4$	$6.7\cdot10^4$	$6.0\cdot10^5$	$1.7\cdot10^6$
SSC	$2.5\cdot10^5$	$1.4\cdot10^5$	$1.9\cdot10^5$	$1.0\cdot10^5$	$2.0\cdot10^5$	$1.8\cdot10^6$	$1.7\cdot10^7$

number of hard muons produced for each extracted accelerator bunch (for the UNK we take the number of bunches to be $N_B = 110$):

$$N_\mu = \frac{N_p}{N_B}\left(\frac{\sigma_c}{\sigma_{tot}}\right)_{bd}\langle BR(c\to\mu)\rangle \simeq 3.4\cdot10^8.$$

These estimates show that it is in principle possible to use the UNK collider to carry out neutrino experiments with reasonable statistics of $\sim 10^5$ events per year at energies not accessible to existing accelerators with fixed targets.

[1)] Part I. See: P. S. Isaev and V. A. Tsarev, Fiz. Elem. Chastits At. Yadra **20**, 997 (1989) [Sov. J. Part. Nucl. **20**, 419 (1989)].
[2)] See: Part I, Eq. (1).
[3)] See also Tables VI and VII and Fig. 14 of Part I.
[4)] These restrictions on the masses of the gauge bosons, which follow from the radiative corrections, were also discussed in the first part of our review.
[5)] If the spectrum of the charmed particles is $dN/dx \sim (1-x)^n$, then their mean energy is $\langle E_c\rangle \simeq E_p/(n+2)$, where E_p is the energy of the primary protons in the laboratory system.

[1]A. M. Baldin, Fiz. Elem. Chastits At. Yadra **8**, 429 (1977) [Sov. J. Part. Nucl. **8**, 175 (1977)]; *Proc. of the 18th Intern. Conf. on High Energy Physics, Tbilisi, 1976*, JINR, Dubna, 1977), p. AG-3.
[2]M. I. Strikman and L. L. Frankfurt, Fiz. Elem. Chastits At. Yadra **11**, 571 (1980) [Sov. J. Part Nucl. **11**, 221 (1980)].
[3]J. Guy, B. Saitta, G. Van Apeldoorn *et al.*, Z. Phys. C **36**, 337 (1987).
[4]J. Ashman, B. Badelek, G. Baum *et al.*, Phys. Lett. **202B**, 603 (1988).
[5]N. N. Nikolaev and V. I. Zakharov, Phys. Lett. **55B**, 397 (1975); Yad. Fiz. **21**, 434 (1975) [Sov. J. Nucl. Phys. **21**, 227 (1975)].
[6]E. L. Berger and J. Qiu, Phys. Lett. **206B**, 141 (1988).
[7]R. L. Jaffe, Phys. Rev. Lett. **50**, 228 (1983); A. V. Efremov and E. A. Bondarchenko, Preprint E2-84-124, JINR, Dubna (1984).
[8]F. E. Close, R. G. Roberts, and G. G. Ross, Phys. Lett. **168B**, 400 (1986).
[9]T. Kitagaki, S. Tanaka, A. Yamaguchi *et al.*, Phys. Lett. **214B**, 281 (1988).
[10]N. P. Zotov, V. A. Saleev, and V. A. Tsarev, Pis'ma Zh. Eksp. Teor. Fiz. **40**, 200 (1984) [JETP Lett. **40**, 965 (1984)].
[11]E. S. Golubyatnikova, B. N. Kalinkin, and V. L. Shmonin, Preprints R2-86-182, R2-86-183 [in Russian], JINR, Dubna (1986).
[12]N. P. Zotov, V. A. Saleev, and V. A. Tsarev, Yad. Fiz. **45**, 561 (1987) [Sov. J. Nucl. Phys. **45**, 352 (1987)].
[13]V. I. Efremenko, A. V. Fedotov, P. A. Gorichev *et al.*, Phys. Rev. D **22**, 2581 (1980); J. P. Berge, D. Bogert, R. Endfort *et al.*, Phys. Rev. D **18**, 1367 (1978).
[14]V. V. Ammosov, D. S. Baranov, A. A. Grobish *et al.*, Yad. Fiz. **43**, 1186 (1986) [Sov. J. Nucl. Phys. **43**, 759 (1986)].
[15]O. V. Kancheli, Pis'ma Zh. Eksp. Teor. Fiz. **18**, 465 (1973). [JETP Lett. **18**, 274 (1973)].
[16]I. Ya. Teplitskiĭ, Preprint No. 1078 [in Russian], Leningrad Institute of Nuclear Physics, Leningrad (1985).
[17]D. S. Baranov, V. I. Ermolaev, A. Ya. Ivanilov *et al.*, Yad. Fiz. **40**, 1454 (1984) [Sov. J. Nucl. Phys. **40**, 923 (1984)].
[18]Yu. M. Shabel'skiĭ, in *Proc. of the 12th Winter School of the Leningrad Institute of Nuclear Physics*, Vol. 1 (1978), p. 90; A. V. Vaĭsenberg, Yu. B. Lepikhin, V. A. Smirnitskiĭ *et al.*, Pis'ma Zh. Eksp. Teor. Fiz. **29**, 719 (1979) [JETP Lett. **29**, 661 (1979)]; B. Slowinski, A. Tomaszewicz, E. Mulas, and W. Czaj, Yad. Fiz. **30**, 173 (1979) [Sov. J. Nucl. Phys. **30**, 89 (1979)]; Yu. M. Shabel'skiĭ and B. S. Yuldashev, Yad. Fiz. **31**, 1646 (1980) [Sov. J. Nucl. Phys. **31**, 854 (1980)].
[19]S. M. Eliseev and B. S. Yuldashev, Preprint R2-82-323 [in Russian], JINR, Dubna (1983).
[20]N. N. Nikolaev, Z. Phys. C **5**, 291 (1980); S. A. Voloshin, Yu. P. Nikitin, and P. I. Porfirov, Yad. Fiz. **31**, 762 (1980) [Sov. J. Nucl. Phys. **31**, 395 (1980)].
[21]D. Antreasyan, J. W. Cronin, H. J. Frisch *et al.*, Phys. Rev. D **19**, 764 (1979).
[22]M. Lev and B. Peterson, Z. Phys. C **21**, 155 (1983).
[23]V. Sukhatme and G. Wiik, Phys. Rev. D **25**, 1978 (1982).
[24]R. Gomez, L. Dauwe, H. Haggerty *et al.*, Phys. Rev. D **35**, 2736 (1987).
[25]H. P. Nilles, Phys. Rep. **110**, 1 (1984); H. E. Haber and G. L. Kane, Phys. Rep. **117**, 75 (1985); L. E. Ibanez and G. G. Ross, Phys. Lett. **110B**, 215 (1982).
[26]S. Dimopoulos and J. Ellis, Nucl. Phys. **B182**, 505 (1981); G. G. Ross, in *International Symposium on Lepton and Photon Interactions at High Energy, Hamburg, 27–31 July, 1987*, edited by W. Bartel and R. Rücke (North-Holland, Amsterdam, 1987), p. 743.
[27]P. Fayet, in *Unification of the Fundamental Particle Interactions*, edited by S. Ferrata, J. Ellis, and P. van Nieuwenhuizen (Plenum Press, New York, 1980), p. 587.
[28]J. Ellis, J. S. Hagelin, D. V. Nanopoulos *et al.*, Nucl. Phys. **B24**, 453 (1984).
[29]J. Ellis and F. Pauss, Preprint CERN TH 2992/88 (1988).
[30]L. E. Ibanez, Phys. Lett. **137B**, 160 (1984).
[31]T. Devlin, in, *Proc. of the 24th International Conference on High Energy Physics, Munich, August 4–10, 1988* (Springer, Berlin, 1989), p. 1459.
[32]H.-J. Beherend, J. Burger, L. Criegee *et al.*, Z. Phys. C **35**, 181 (1987).
[33]M. Gell-Mann, P. Ramoud, and R. Slansky in *Supergravity*, edited by P. van Nieuwenhuizen and D. Freedman (North-Holland, Amsterdam, 1979), p. 186; R. N. Mohaparta and G. Senjanović, Phys. Rev. Lett. **44**, 912 (1980).
[34]A. Davidson and K. Wali, Phys. Lett. **98B**, 183 (1981); E. Papantonopoulos and G. Zoupanos, Phys. Lett. **110B**, 465 (1982); J. Bagger, S. Dimopoulos, E. Masso, and M. H. Reno, Phys. Rev. Lett. **54**, 2199 (1985); Nucl. Phys. **B258**, 565 (1985).
[35]P. S. Isaev and S. G. Kovalenko, in *Proc. of the Eighth Working Symposium on the IHEP–JINR Neutrino Detector*, D1,2, 13-88-90 [in Russian] (Dubna, 1988), p. 135.
[36]M. Gronau, C. N. Leung, and J. L. Rosner, Phys. Rev. D **29**, 2539 (1984).
[37]S. A. Bunyatov, O. Yu. Denisov, V. S. Kurbatov, and A. A. Osipov, in *Proc. of the Eighth Working Symposium on the IHEP–JINR Neutrino Detector*, R1,2,13-86-508 [in Russian] (Dubna, 1986), p. 5.
[38]J. Dorenbosch, J. V. Allaby, U. Amaldi *et al.*, Phys. Lett. **166B**, 473 (1986).
[39]S. T. Petkov, Yad. Fiz. **25**, 641, 1336(E) (1977) [Sov. J. Nucl. Phys. **25**, 340, 698(E) (1977)]; L. Pal'gi in *Proc. of the Eighth Working Symposium on the IHEP–JINR Neutrino Detector*, R1,2,13-86-508 [in Russian] (Dubna, 1986), p. 14.
[40]J. F. Nieves, Phys. Rev. D **28**, 1664 (1983).
[41]R. K. Ghosh, Phys. Rev. D **29**, 493 (1984).
[42]B. W. Lee and R. E. Shrock, Phys. Rev. D **16**, 1444 (1977); W. J. Marciano and A. J. Sanda, Phys. Lett. **67B**, 303 (1977).
[43]B. Pal and L. Wolfenstein, Phys. Rev. D **25**, 766 (1982); J. Nieves, Phys. Rev. D **26**, 3152 (1982).
[44]S. L. Glashow, J. Iliopoulos, and L. Maiani, Phys. Rev. D **2**, 1285 (1970).
[45]O. Yu. Denisov and V. S. Kurbatov, in *Proc. of the Eighth Working Symposium on the IHEP–JINR Neutrino Detector*, R1,2,13-86-508 [in Russian] (Dubna, 1986), p. 23.
[46]R. E. Shrock, Phys. Rev. D **24**, 1232 (1981).
[47]G. Bernardi, G. Carugno, J. Chauvean *et al.*, Phys. Lett. **266B**, 479 (1986).
[48]R. Eichler, in *International Symposium on Lepton and Photon Interactions at High Energies, Hamburg, 27–31 July, 1987*, edited by W. Bartel and R. Rücke (North-Holland, Amsterdam, 1987), p. 389.
[49]F. Bergsma, J. Dorenbosch, M. Jonner *et al.*, Phys. Lett. **128B**, 361

(1983).
[50]A. M. Cooper-Sarkar, S. J. Haywood, M. A. Parker *et al.*, Phys. Lett. **160B**, 207 (1985).
[51]I. Blyumleĭn, M. Val'ter, and K. Shpiring, in *Proc. of the Eighth Working Symposium on the IHEP–JINR Neutrino Detector*, D1,2,13-88-90 [in Russian] (Dubna, 1988), p. 6.
[52]*Neutrino 86. Proc. of the 12th International Conference on Neutrino Physics and Astrophysics, Sendai, June 3–8, 1986*, edited by T. Kitagaki and H. Yuta (World Scientific, Singapore, 1986).
[53]*Proc. of the Sixth Moriond Workshop on Massive Neutrinos in Astrophysics and in Particle Physics*, edited by O. Fackler and J. Tran Thanh Van (Éditions Frontières, 1986).
[54]P. S. Isaev and I. S. Zlatev, Preprint D2-81-287 [in Russian], JINR, Dubna (1981).
[55]G. Steigman, K. A. Olive, D. N. Schramm, and M. S. Turner, Phys. Lett. **176B**, 33 (1986); J. Ellis, K. Enqvist, D. V. Nanopoulos, and S. Sarkar, Phys. Lett. **167B**, 457 (1986).
[56]J. Ellis and K. Olive, Phys. Lett. **193B**, 525 (1987); M. Davier, in *Proc. of the 23rd International Conference on High Energy Physics, Berkeley, 1986*, edited by S. C. Loken (World Scientific, Singapore, 1987), p. 25.
[57]M. Gronau, C. N. Leung, and J. L. Rosner, Phys. Rev. D **29**, 2539 (1984).
[58]V. Barger and R. J. N. Phillips, Phys. Lett. **198B**, 473 (1987).
[59]J. Ellis and F. Pauss, Preprint CERN TH 4992/88, march (1988).
[60]C. Albair, M. G. Albrow, O. C. Allkofer *et al.*, Phys. Lett. **185B**, 241 (1987).
[61]M. Mohammadi, Thesis, University of Michigan, Madison (1987).
[62]M. S. Chanowitz, Preprint LBL-24878, February (1988).
[63]U. Amaldi, A. Rohin, L. S. Durkin *et al.*, Phys. Rev. D **36**, 1385 (1987).
[64]S. Komamiya, in *Proc. of the 1985 International Symposium on Lepton and Photon Interactions at High Energy* (Kyoto, August 19–24, 1985), p. 612.
[65]S. Behrends *et al.*, Cornell Preprint CLNS 87/88, July (1987).
[66]B. W. Lee, C. Quigg, and H. B. Tacker, Phys. Rev. D **16**, 1519 (1977).
[67]M. Drees, M. Klück, and W. Grassie, Phys. Lett. **159B**, 118 (1985); E. Reya, Phys. Rev. D **33**, 773 (1986).
[68]G. G. Athanasiu, P. J. Franzini, and F. J. Gilman, Phys. Rev. D **32**, 3010 (1985).
[69]H. J. Berends, J. Bürger, L. Criegee *et al.*, Phys. Lett. **193B**, 376 (1987).
[70]S. L. Wu, in *International Symposium on Lepton and Photon Interactions at High Energies, Hamburg, 27–31 July, 1987*, edited by W. Bartel and R. Rücke (North-Holland, Amsterdam, 1987), p. 39.
[71]H. Georgi, S. L. Glashow, M. Machacek, and D. L. Nanopoulos, Phys. Rev. Lett. **40**, 692 (1978).
[72]Yu. P. Ivanov and A. M. Rozhdestvenskiĭ, in *Proc. of the Eighth Working Symposium on the IHEP–JINR Neutrino Detector*, R1,2,13-83-81 [in Russian] (Dubna, 1983), p. 120.
[73]J. Panman, in *Proc. of the 1987 International Symposium on Lepton and Photon Interactions at High Energies, Hamburg, 27–31 July, 1987*, edited by W. Bartel and R. Rücke (North-Holland, Amsterdam, 1987), p. 553.
[74]C. H. Albright, J. Smith, and J. A. M. Vermaseren, Phys. Rev. D **18**, 108 (1978).
[75]F. Niebergall, in *Proc. of the International Conference on Neutrino Physics and Astrophysics (Neutrino 82), 14–19 June, 1982, Balatonfured, Hungary*, edited by A. Frenkel and L. Jenik (Budapest, 1982), N2, p. 62.
[76]J. C. Pati and A. Salam, Phys. Rev. Lett. **31**, 661 (1973); Phys. Rev. D **10**, 275 (1974).
[77]A. Jodidio, B. Balke, J. Carr *et al.*, Phys. Rev. D **34**, 1967 (1986).
[78]J. Carr, G. Gidal, B. Gobbi *et al.*, Phys. Rev. Lett. **51**, 627 (1983).
[79]P. Langacker, R. A. Robinett, and J. L. Rosner, Phys. Rev. D **30**, 1470 (1984).
[80]L. S. Durkin and P. Langacker, Phys. Lett. **116B**, 436 (1986).
[81]V. A. Bednyakov and S. G. Kovalenko, Phys. lett. **214B**, 640 (1988); Yad. Fiz. **49**, 866 (1989) [Sov. J. Nucl. Phys. **49**, 538 (1989)].
[82]E. Eichten, I. Hinchliffe, K. Zane, and C. Quigg, Rev. Mod. Phys. **56**, 579 (1984).
[83]R. Ansari, P. Bagnaia, M. Banner *et al.*, Phys. Lett. **195B**, 613 (1987).
[84]G. Arnison, M. G. Albrow, O. C. Allkofer *et al.*, Europhys. Lett. **1**, 327 (1986).
[85]C. Hearty, J. E. Rothberg, K. K. Young *et al.*, Phys. Rev. Lett. **58**, 1711 (1987).
[86]W. T. Ford, N. Qi, A. L. Read *et al.*, Phys. Rev. D **33**, 3472 (1986).
[87]L. Gladney, R. J. Hollenbeek, B. W. LeClaire *et al.*, Phys. Rev. Lett. **51**, 2253 (1983).
[88]B. Naroska, Phys. Rep. **148**, 67 (1987).
[89]MARK-I Collaboration, in *Proc. of the 1987 International Symposium on Lepton and Photon Interactions at High Energies, Hamburg, 27–31 July, 1987*, edited by W. Bartel and R. Rücke (North-Holland, Amsterdam, 1987).
[90]R. Brandelik, W. Braunschweig, K. Gather *et al.*, Phys. Lett. **117B**, 365 (1982).
[91]B. M. Pontecorvo, Zh. Eksp. Teor. Fiz. **33**, 549 (1957) [Sov. Phys. JETP **6**, 429 (1958)]; S. M. Bilen'kiĭ and B. M. Pontecorvo, Usp. Fiz. Nauk **123**, 181 (1977) [Sov. Phys. Usp. **20**, 776 (1977)].
[92]S. M. Bilen'kiĭ, Fiz. Elem. Chastits At. Yadra **18**, 449 (1987) [Sov. J. Part. Nucl. **18**, 188 (1987)].
[93]S. M. Bilenky and S. T. Petcov, Rev. Mod. Phys. **59**, 671 (1987).
[94]L. B. Okun, Neutrino 88 Conference, Boston, MA June 5–12 (1988).
[95]D. L. Chkaureli, Pis'ma Zh. Eksp. Teor. Fiz. **32**, 684 (1980) [JETP Lett. **32**, 671 (1980)].
[96]Z. G. Berezhiani and D. L. Chkaureli, Pis'ma Zh. Eksp. Teor. Fiz. **37**, 285 (1983) [JETP Lett. **37**, 338 (1983)].
[97]Z. G. Berezhiani and J. L. Chkareuli, in *Proc. of the Workshop on Experimental Program at UNK* (Protvino, 1987), p. 91.
[98]L. Wolfenstein, Phys. Rev. D **17**, 2369 (1978).
[99]S. P. Mikheev and A. Yu. Smirnov, Usp. Fiz. Nauk **153**, 3 (1987) [Sov. Phys. Usp. **30**, 759 (1987)].
[100]S. P. Denisov, V. P. Zhigunov, S. A. Mukhin *et al.*, in *Proc. of the Working Symposium: Physics Investigations with the IHEP UNK* [in Russian] (Protvino, 1982), p. 167.
[101]V. A. Tsarev in *Proc. of the Working Symposium on the Program of Experimental Investigations with the UNK* [in Russian] (Protvino, 1987), p. 118.
[102]V. A. Tsarev and V. A. Chechin, Fiz. Elem. Chastits At. Yadra **17**, 389 (1986) [Sov. J. Part. Nucl. **17**, 167 (1986)].
[103]L. V. Volkova and G. T. Zatsepin, Izv. Akad. Nauk. SSSR, Ser. Fiz. **38**, 1060 (1974).
[104]I. P. Nedyalkov, Preprints 18-81-189, R2-81-645 [in Russian], JINR, Dubna (1981).
[105]A. De Rújula, S. L. Glashow, R. R. Wilson *et al.*, Phys. Rep. **99**, 341 (1983).
[106]L. V. Volkova, Nuovo Cimento **86**, 552 (1985).
[107]V. A. Tsarev and V. A. Chechin, Fiz. Zemli **9**, 81 (1986).
[108]D. S. Baranov, B. S. Volkov, S. S. Gershteĭn *et al.*, Preprint 83-87 [in Russian], Institute of High Energy Physics (1983).
[109]V. A. Tsarev, Kratk. Soobshch. Fiz. **11**, 48 (1985); V. K. Ermilova, V. A. Tsarev, and V. A. Chechin, Preprint No. 45 [in Russian], P. N. Lebedev Physics Institute (1986); Preprint No. 218 [in Russian], P. N. Lebedev Physics Institute (1988); Pis'ma Zh. Eksp. Teor. Fiz. **43**, 353 1986) [JETP Lett. **43**, 453 (1986)].
[110]P. I. Krastev and S. T. Petcov, Phys. Lett. **205B**, 84 (1988).
[111]T. K. Kuo and J. Pantaleone, Purdue Preprint PURD-TH-87-12 (1987).
[112]V. K. Ermilova, V. A. Tsarev, and V. A. Chechin, Kratk. Soobshch. Fiz. **3**, 38 (1988).
[113]V. Barger, K. Whisnant, and R. J. N. Phillips, Phys. Rev. Lett. **45**, 2084 (1980); Phys. Rev. D **23**, 2773 (1981).
[114]V. N. Zharkov, *Internal Structure of the Earth and the Planets* [in Russian] (Nauka, Moscow, 1983).
[115]N. Z. Gogitidze, V. A. Tsarev, and V. A. Chechin, Preprints Nos. 94, 216, 225 [in Russian], P. N. Lebedev Physics Institute (1984, 1988, 1988); N. Z. Gogitidze *et al.*, Nucl. Instrum. Methods **A248**, 186 (1986).
[116]S. M. Bilenki, J. Hosek, and S. T. Petcov, Phys. Lett. **94B**, 495 (1980).
[117]P. Langacker, S. T. Petcov, G. Steigman, and S. Toshev, Nucl. Phys. **B282**, 589 (1987).
[118]Z. G. Berezhiani and M. I. Vysotsky, Phys. lett. **199**, 281 (1987).
[119]G. B. Gelmini and M. Roncadelli, Phys. Lett. **99B**, 411 (1981).
[120]E. V. Kolomeets, V. S. Murzin, Dzh. Al'bers *et al.*, "The batiss experiment," in *Proc. of the First All-Union Conference: Investigation of Muons and Neutrinos in Large Water Volumes, Alma-Ata, 1983* [in Russian] (Kazakh State University, 1983), p. 16.
[121]R. Böstrom *et al.*, *Proc. of the 16th International Cosmic Ray Conference*, Vol. 10 (Kyoto, 1976), p. 266.
[122]V. A. Saleev, V. A. Tsarev, and V. A. Chechin, Kratk. Soobshch. Fiz. **7**, 49 (1985).
[123]G. A. Askar'yan, At. Energ. **3**, 152 (1957); G. A. Askar'yan and B. A. Dolgoshein, Pis'ma Zh. Eksp. Teor. Fiz. **25**, 232 (1977) [JETP Lett. **25**, 231 (1977)].
[124]O. B. Khavroshkin, V. A. Tsarev, V. V. Tsyplakov, and V. A. Chechin, Kratk. Soobshch. Fiz. **10**, 26 (1985); Preprint No. 167 [in Russian], P. N. Lebedev Physics Institute (1985).
[125]G. A. Askar'yan, Zh. Eksp. Teor. Fiz. **41**, 616 (1961); **48**, 985 (1965) [Sov. Phys. JETP **14**, 441 (1962); **21**, 656 (1965)]; Pis'ma Zh. Eksp. Teor. Fiz. **39**, 334 (1984) [JETP Lett. **39**, 402 (1984)].
[126]V. A. Tsarev and V. A. Chechin, Preprints Nos. 248, 87 [in Russian], P. N. Lebedev Physics Institute (1984, 1985).
[127]S. I. Nikol'skiĭ and V. A. Tsarev, Kratk. Soobshch. Fiz. **1**, 57 (1984).
[128]A. De Rújula and R. Ruckl, in *Proc. of the Workshop on the Feasibility of Hadron Colliders in the LEP Tunnel* (Lausanne and CERN, March,

1984).
[129]N. P. Zotov, V. A. Saleev, V. A. Tsarev, and V. A. Chechin, Pis'ma Zh. Eksp. Teor. Fiz. **39**, 81 (1984) [JETP Lett. **39**, 97 (1984)].
[130]N. P. Zotov and V. A. Tsarev, Kratk. Soobshch. Fiz. **12**, 19 (1987).

Translated by Julian B. Barbour